Gait stability assessment during perturbed walking

By

Hosein Bahari

A thesis submitted in partial fulfillment of the requirements for the degree of

Master of Science

Department of Mechanical Engineering
University of Alberta

Abstract

Falling is a significant source of morbidity and even mortality among the elderly population. 10% to 20% of these falls lead to severe injuries that require medical attention. Understanding the mechanisms behind the loss-of-balance and fall initiation can help prevent the consequences of falls by designing preventive strategies and training to help individuals maintain their balance. Over 50% of falls occur during locomotion. The risk of falling during walking has been assessed using stability measures based on either the dynamic stability of the system or the biomechanical modeling of the human body. The former approach is better suited for balance assessment during unperturbed walking whereas the latter is suitable for both perturbed and unperturbed walking circumstances. The biomechanical mechanisms behind the loss-of-balance and falling during walking have been studied for the cases of slip and non-slip conditions. However, they have not been studied for the complex perturbation scenarios.

The objectives of this study were to, first, characterize the biomechanical mechanisms of loss-of-balance during perturbed walking as a function of perturbation conditions, body motion patterns, and gait parameters, and second, propose and experimentally validate stability measures for perturbed walking conditions.

We used a seven-segment model of the human body and presented a non-linear, optimization-based model of perturbed walking in the sagittal plane. We analyzed human body motions during swing phase of walking and quantified the effects of various types of external perturbations on the base of support (BOS) on the walking stability. We estimated the boundaries (limits) of the feasible stability region (FSR) as a function of the type, dominant frequency, and dominant amplitude of perturbations. To extend the use of obtained FSRs to continuous perturbed or unperturbed walking,

we introduced the concept of "extended feasible stability region" (ExFSR) which included the region between the leading foot's lower FSR threshold and swinging foot's upper FSR threshold. Based on this concept, we introduced novel stability measures for a whole step duration in a walking trial.

To experimentally validate our obtained feasible stability regions and proposed stability measures, we collected experimental data from two groups of nondisabled individuals and individuals with disability during perturbed walking. To this end, we used a Computer-Assisted Rehabilitation Environment (CAREN) to create various perturbation conditions. We evaluated the validity of the obtained feasible stability regions at the toe-off instant and ExFSR during a whole step duration by investigating their specificity in predicting the loss-of-balance (i.e., false prediction of the loss-of-balance). The specificity of obtained feasible stability regions and ExFSR were comparable to those reported in the literature for other conditions. Also, we evaluated the credibility of our proposed stability measures by showing their correlation with other biomechanical and variability-based stability measures previously introduced in the literature.

This study introduced biomechanical measures to characterize the risk of loss-of-balance in the sagittal plane during perturbed walking as a function of perturbation conditions, body motion patterns, and gait parameters. These measures can be used for physiologically and biomechanically meaningful assessment of walking stability for individuals with walking disorders. The outcome of this research can contribute to our understanding of human balance control for biped walking under the effect of external perturbations, and the development of rehabilitative programs in interactive training environments such as the CAREN.

Keywords: Dynamic optimization; Fall prevention; Forward dynamics; Musculoskeletal modeling; Walking stability; Computational biomechanics; Stability measure

Preface

This thesis is an original work by Hosein Bahari. The research project, of which this thesis is a part of, received research ethical approval from the local research ethics board (protocol number: Pro00066076).

Chapter 3 of this research has been submitted as an original article (research paper) to the *Journal of biomechanics*, titled as "**predicted threshold against forward and backward loss of balance for perturbed walking**".

Chapter 4 of this research has been submitted as an original article (research paper) to the *Journal of biomechanics*, titled as "**Extended feasible stability region: An approach to assess stability of perturbed walking**".

Chapters 3 and 4 of this thesis present a methodology, data analysis and interpretation of collected experimental data that are the original contribution of Hosein Bahari. Experimental data were collected by our research team using the research facility of the Glenrose rehabilitation hospital. The application for Research Ethics Board permission was originally written by Mr. Juan Forero and the experimental protocol was designed and executed by Juan Forero with the help of Hosein Bahari and Jeremy Hall under supervision of Drs. Jaqueline Hebert and Albert Vette.

Parts of this thesis were presented as two posters at the *Spotlight on Research 2017* and *Spotlight on Innovation (2018)* (Hosted by Glenrose rehabilitation hospital, Edmonton, Canada) and a presentation at the *19th annual biomedical engineering conference 2018* (Banff, Canada).

Dedicated to

my brother,

Hamed Bahari

Acknowledgments

I would like to show my sincere gratitude to my supervisor, Hosein Rouhani, who treated me as student, friend and a younger brother and never hesitated in helping and elevating me. I would like to thank him for his guidance, encouragement, dedication, patience, hard work and I would like to appriciate all his efforts towards making me a more succesful person in life.

I would like to thank my parents and my brother who always inspired me, supported me and showed me the correct path. I would like to thank the love of my life, Ladan Ansarimehr, who always stood by my side when I needed her the most and never stopped beliving in us. I would like to thank my friends, Azin Moshir, Reyhane Taghipour, Alireza Moayyedi, Mohsen Safaei, Keyhan Babaei, Ali Pourzahedi, Mehryar Keshavarz, Andy Williams, Jeremy Hall and Hossein Jafari who where always there for me when I needed help and friendship. I would like to thank Drs. Juan Forero , Albert Vette, Jaqueline Hebert and Mr. Darrel Goertzen for contributing in my research and helping me with performing my experiments and providing guidance for writing my papers. I would like to thank my labmates, Milad Nazar Ahari, Alireza Noamani, Niloufar Ahmadian, Ramin Fathian and Aminreza Khandan who I could always count on and helped me along the way. Lastly, I would like to thank Jim Raso for his understanding and having me at the Glenrose rehabilitation hospital's research building.

This project was made possible through the generous support of the Faculty of Engineering of the University of Alberta, the Faculty of Graduate Studies and Research, Glenrose Rehabilitation hospital, and the Natural Sciences and Engineering Research Council of Canada.

Table of Contents

List of Tables

List of Figures

acceleration; *bh*: body height), respectively. Values of 0 and –1 on the horizontal axis indicate the location of the right toe and heel, respectively. These limits (shown as red lines) are compared to those obtained by Pai et al. [8] and Yang et al. [78] for non-slip conditions that used a different number of segments and/or optimization cost function.

Figure 8: Effects of frequency and amplitude of the perturbations on the limits of the feasible stability range (FSR). Plots (a) to (e) show the FSR limits when the base of support (BOS) perturbations are modeled as sinusoidal movements in the vertical direction, and plots (f) to (j) show the FSR limits when BOS perturbations are modeled as a sinusoidal rotation between right foot and the horizontal plane. The center of mass (COM) position and velocity are normalized as in Figure 7.

Figure 9: COM position and velocity obtained experimentally for two walking trials of one representative non-disabled participant (+ points) and one case of participant (Δ points) with amputation (feasible stability limits, FSR, obtained through simulation results). + and Δ Points illustrate right foot lift-off instances. The top graph is representative of the walking trial with low perturbation intensity (vertical displacements and sagittal rotations with frequency of 1 Hz and amplitudes of ±1cm and ±0.6º, respectively), and the bottom graph is representative of the walking trial with high perturbation intensity (vertical displacements and sagittal rotations with frequency of 3 Hz and amplitudes of ±6 cm and ±3º, respectively)

Figure 10: Illustration of optimization and simulation process used to obtain the Feasible Stability Region (FSR) limits for perturbed walking conditions. The output of the optimization process is the maximum and minimum feasible normalized COM velocity for every initial COM position.

Figure 11: Extended Feasible Stability Region (ExFSR), along with the body's COM motion trajectory for the duration of one foot's toe-off instant to the next foot's toe-off instant (one complete swing phase and the following double-support phase). ExFSR region has been marked with transparent dashed lines. The shortest distance between the COM motion trajectory and the lower and upper limits of ExFSR ($M_L(n)$ and $M_U(n)$) was measured as the stability measure. LF, SF and SL stand for standing foot, swinging foot, and step length, respectively.

Figure 12: Stability measures obtained using experimental data. Our proposed measures ($M_{L,avg}$, $M_{U,avg}$, $M_{L,neg,}$ $M_{,U,neg,}$ M_{neg}), XCOM-based biomechanical measure ($b_{min,avg}$), and variability measures (GCT_{nMAD}, GCT_{MAD}, SPP_{nMAD}, and SPP_{MAD}) are presented for non-disabled participants (circle) and participants with disability (triangle), for low-perturbation (L_p, red) and high-perturbation (H_p, dark blue) walking trials.

Figure A1: Schematic of ground reaction force modelling approach. Vertical arrows are indicative of spring-damper elements and their corresponding vertical force. Elements were spaced equally throughout the length of foot.

Nomenclature

3D	Three-dimensional
BOS	Base of Support
CG	Centre of Gravity
COM	Center of Mass
COP	Center of Pressure
CV	Coefficient of Variation
ExFSR	Extended Feasible Stability Region
FSR	Feasible Stability Region
GCT	Gait Cycle Time
GRF	Ground Reaction Force
HAT	Head-Arms-Trunk
I	Inertia
L	left
L_e	Equivalent Trochantric length
LF	Left Foot
M	ExFSR-based stability measure
MAD	Median Absolute Deviation
nMAD	Normalized Median Absolute Deviation

R	Right
RF	Right Foot
RMS	Root Mean Square
ROM	Range of Motion
SPP	Swing Phase Percentage

Chapter 1

1 Introduction

Falls are a leading cause of severe injuries and death for the elderly population [1]. Fall-related injuries can lead to long-term disability, decreased quality of life, and premature death [2]. About 180,000 injurious falls of the senior citizens are annually reported in Canada [3]. In 2004, the direct costs related to falls among older adults in Canada was estimated to be over 2 billion dollars [4].

A significant and consistent predictor of future falls is gait and balance impairment [5]. The majority of falls occur during locomotion and gait [6]. Walking is one of the most integral daily activities of a human being. Stability is a critical element in both standing and walking dynamics [7]. The neuromuscular control system maintains balance of the human body. Yet we do not possess enough knowledge of how this control system maintains the walking balance, and how its functioning can deteriorate due to aging and neurological conditions [8].

A critical step in falling prevention is to assess the risk of falling and identify the individuals with a high risk of falling. Researchers have long studied stability of human gait and the relation between gait stability, stability measures, and risk of falling [9]. Stability measures can either be based on the mathematical properties of the time-series expressing the kinematic parameters or the biomechanics of human movement [12]. On one hand, mathematical tools such as Maximum Floquet multiplier [10], Maximum Lyapunov exponent [11], Poincare mapping [12], and standard deviation of gait parameters [13] have been utilized to assess the variability of gait parameters and relate this variability to the risk of falling. On the other hand, biomechanical models were developed to characterize and quantify the dynamic stability of the human body during gait [8], [14]. Tools, such as extrapolated centre of mass (XCOM) [15] and feasible stability region (FSR) [16] were defined to identify possible combinations of COM position and COM velocities (hereafter referred to as 'COM states') that enabled the walking balance. The simplest method for modeling the human body is the two-segment inverted pendulum model [8]. More complex

biomechanical model were developed throughout the literature [17]–[19] (Figure 1). Notably, the computational cost increases with the model's complexity, and thus a trade-off for simplicity of the modeling approach used for practical application is inevitable.

There exist several differences between stability measures based on the variability of dynamical system and those based on the biomechanical models. As discussed in Chapter 2, the variability measures cannot quantitatively separate the effects of intrinsic variability of walking dynamics and the variability due to external perturbations [9] on the risk of loss-of-balance. Therefore, the extent to which variability measures are reliable for balance assessment during perturbed walking is a matter of debate [20]. However, biomechanical modeling of human gait allows us to quantitatively model external perturbations and their effect on the gait pattern and the risk of loss-of-balance [21]. Being able to investigate the effects of complex external perturbations on gait stability leads to ability of balance assessment during more natural walking circumstances.

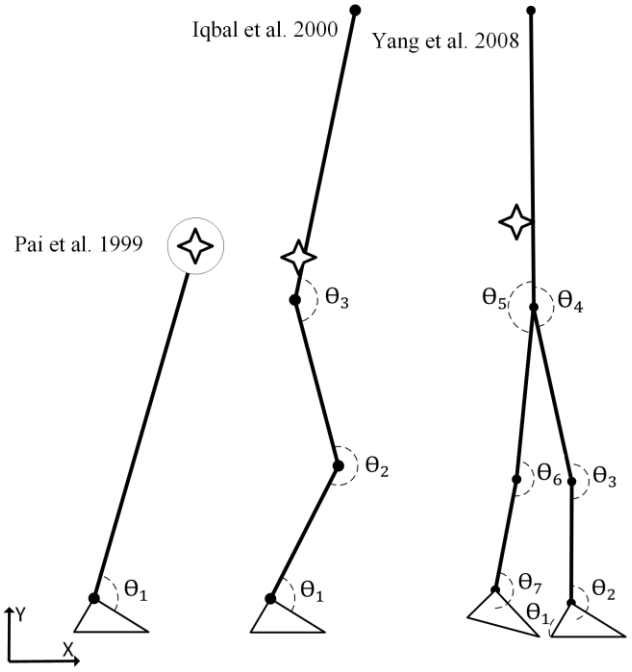

Figure 1: Various biomechanical models (two-segment, four-segment, and seven-segment) developed in the literature to analyze human gait. The inverted pendulum [8], left-side figure, is the simplest approach towards human gait modeling. Four segment [22] and seven segment models [21] are examples of more complex biomechanical models developed to analyze human gait. θ_i indicates the angular position of biological joints and star signs indicate the location of body COM.

Although biomechanical mechanisms of loss-of-balance were investigated for a few perturbation conditions (e.g., slippage), these mechanisms have not been studied for more complex external perturbations, and there is a lack of stability measures based on both biomechanics of gait and external perturbations profile. Such measure can quantify the risk of falling for an individual based on the physiological and biomechanical characteristics of his body. Although several stability measures can be proposed based on various modeling assumptions to take into account multiple factors, the effectiveness and validity of these measures must be experimentally investigated before using them for real-world applications [23] .

The objectives of this study were to, first, characterize the biomechanical mechanisms of loss-of-balance during perturbed walking as a function of perturbation conditions, body motion patterns, and gait parameters, and second, propose and experimentally validated stability measures for perturbed walking conditions.

1.1 Specific aims

To achieve the objectives mentioned above, the specific aims of this research are defined as listed below.

1. Develop a seven-segment model of the human body in the sagittal plane during a swing phase of gait.
2. Using developed biomechanical model, derive the state subspace of the normalized COM velocity versus the normalized COM position in which walking stability is feasible (referred to as FSR), and compare the results with the literature.
3. Impose perturbations to the Base of Support (BOS) of the model and investigate the effects of external perturbations on the limits of FSR (referred to as FSR limits).
4. Introduce the new concept of extended feasible stability region (ExFSR) and its associated stability measure to assess the stability of perturbed walking during a complete step.
5. Collect experimental data from a total of fifteen able-bodied participants and three individuals with walking disabilities, to evaluate the validity of the FSRs, ExFSR, and its associated stability measure.

6. Investigate the correlation between the newly defined stability measure and other existing stability measures in the literature.

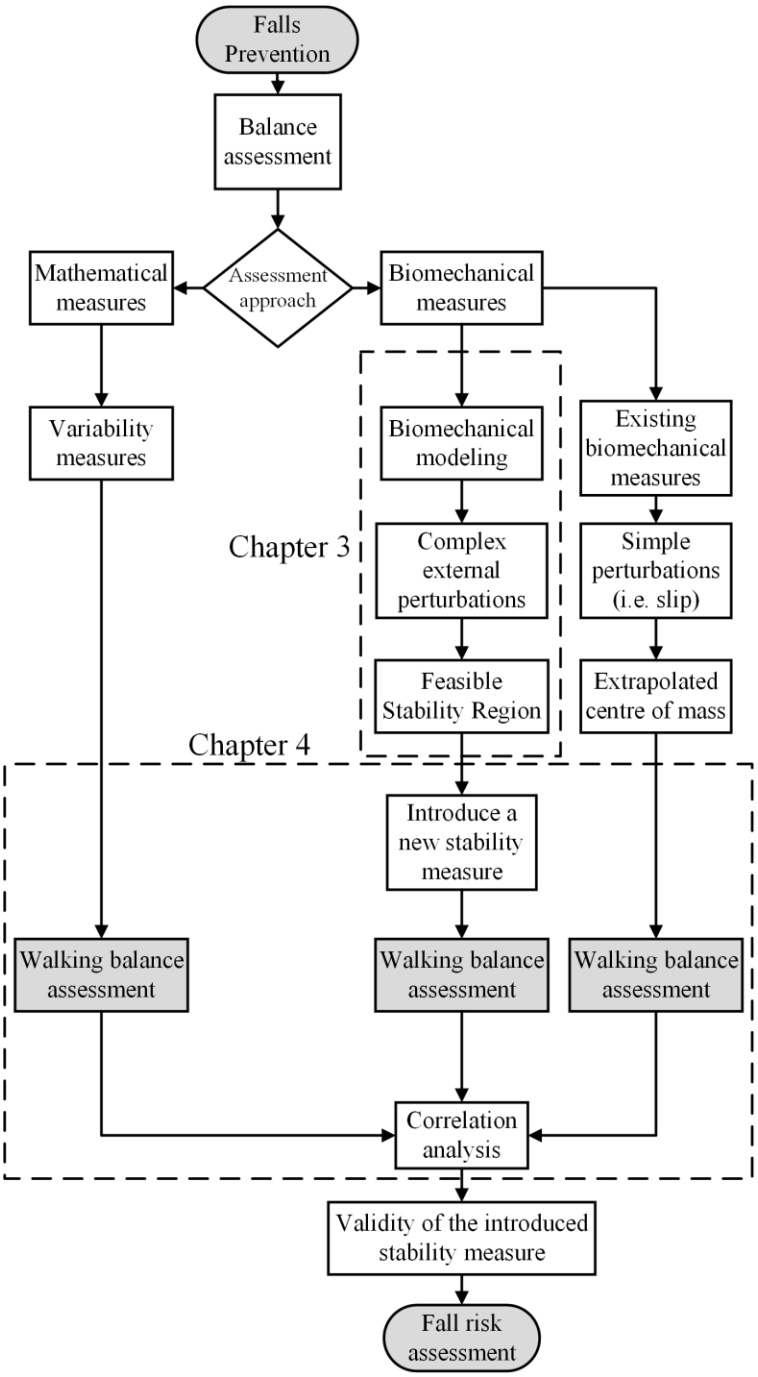

Figure 2: Thesis outline and an overview of the current study and methodology

1.2 Thesis outline

Chapter 2 of this thesis reviews the literature that is relevant to this study: a review of gait and its elements; a review of the definition of balanced gait and the relation between loss-of-balance and incidence of falling; a review of stability region and its definition; a review of dynamics of gait; a review of biomechanical modeling and finally an overview of stability measures and their differences. Chapter 3 describes a novel methodology to obtain the FSR at a time instant during swing phase for perturbed walking circumstances. Chapter 3 also characterizes the FSR as a function of complex perturbation parameters that may occur during daily life. Chapter 4 presents novel stability measures based on the method and model developed in Chapter 3. Chapters 3 and 4 also investigate the validity of the obtained FSR and stability measures using experimental data. Chapter 4 further analyzes the correlations between introduced stability measures and existing stability measures described in the literature. Chapter 5 summarizes the thesis outcome and its original contribution as well as providing conclusive remarks on the present study, and describes the limitation and possible future perspectives (Figure 2).

Chapter 2

2 Literature review

2.1 Normal gait

Normal Gait is a combination of body movements in a progressive way that demands every supporting member of the human body to be alone or in association with another supporting member [24]. Gait patterns change relative to the nature of walker's legs and terrain. Various aspects of the human gait have been studied. The normal and pathological patterns of the ground reaction forces [25], electromyography (EMG) recording patterns and muscle forces [26], [27] kinematics and kinetics of lower limb [17], [28] during gait have been reported. Not all these findings are going to be covered in the present study. This study will look over the dynamics of gait and ground reaction forces during unperturbed and perturbed gait. There are limitations to the experimental study of human gait such as limitations to direct measurement of muscle forces and joint torques non-invasively. Gait can be categorized as a complex motion and finding the governing dynamical equations for complex human models can be a challenge itself.

2.1.1 Elements of Gait

"Walking can be defined as periodic movements of lower limbs which maintain the body in a forward progression on a leveled ground" [25]. A gait cycle consists of two steps and each step consists of a swing (single-support) and a double-stance (double-support) phase. Each swing phase starts with one foot's toe-off instant and ending with the same foot's heel-strike instant. During this time the other foot is in contact with the ground. After each swing phase, there is a double support phase, in which both feet are in contact with the ground surface, and during this time, the weight of the body is transferred from one foot to the other one. The swing phase of each foot takes approximately 40% of a complete gait cycle in normal gait and each of the two double-

support phases takes approximately 10% of a complete gait cycle [29]. A complete gait cycle includes two swing phases and two stance phases.

The two basic requirements of walking are 1) continuous ground reaction force and 2) periodic and repeatable movements [25]. During regular walking, the COM of the whole body follows an oscillatory trajectory in the horizontal plane with a fluctuating COM velocity profile. In the vertical direction, COM goes up and down periodically, but the amplitude of the COM motion fluctuations is smaller compared to the horizontal direction. Due to multiple degrees of freedom of the human body, the COM trajectory during walking is smooth.

Walking elements are defined to be the coordination of different body parts during a natural walking cycle [25]. We will define these elements in this section one by one. The first element, *pelvic rotation,* is defined as the rotation of pelvis in the transverse plane which at normal speed, the amplitude of this rotation is 8 degrees on either side of the vertical axis of the pelvis. The second element, *pelvis list,* is the rotation of pelvis in the sagittal plane and typical amplitude of this rotation is known to be 5 degrees on either side of pelvis axis. The third element, *knee flexion during stance,* is the amount of knee joint's flexion angle in sagittal plane during stance phase, which goes up to 15 degrees. According to Inman et al. [30], the three of these elements are working together to result in a smooth COM trajectory; however, the most essential walking elements are known to be ankle and knee flexion-extension. These two motions are combined as one element called the *knee interaction* [31].

In addition to elements related to the lower limb motion, there is also motion in arms, shoulders, and torso. These motion elements are much less effective compared to lower limb related elements. According to Inman et al. [30], these motions are meant to have balancing effects for the opposite rotations of the pelvis.

Although the predominant motion of body segments during gait are in the sagittal plane, it is important to include those motions in transverse and frontal planes. Most of the biomechanical models presented in the literature only consider lower limb walking elements in the sagittal plane, due to the high computational costs of expanding the degrees of freedom of the body motion to the transverse and frontal planes.

2.2 Kinematics and dynamics of walking

Bipedal locomotion has been defined as the vaulting movement of human body over one stance leg in a way that the body trajectory is stabilized through the movements of the other leg at the end of its swing phase [32]. Dynamical phase plane movements of body segments in the sagittal plane during walking is a crucial element of stability analysis. Kinematic and dynamic analysis of walking aim to obtain the motions of the body segments and joints forces and moments along with the reaction forces acting on the body from external sources.

The most common approach towards biomechanical modeling of the human body is using forward dynamics modeling in conjunction with optimization methods [17], [21]. The high number of segments and joints involved and the complexity of the dynamical system will transform the task of walking into a sophisticated dynamical problem. In predictive models of walking usually, an optimization routine is utilized to predict the movements, forces and moments acting on the system to the end of predicting the final movement of the system [22].

2.3 Biomechanical modeling of walking

Although gait analysis and the efforts taken in its regards have led to a more specific assessment of locomotion and its biomechanics, our ability to perfectly model walking is limited in two respects. First, the human body and musculoskeletal system is a redundant system in term of mechanical solutions because each joint is in contact with several muscles [27]. Second, the behavior of our motor control system and the mechanisms of its decision-making is still unknown to us. Besides, the difficulties of muscle force measurements adds to the issue. There is no flawless path to take for biomechanical modeling of human locomotion, but a sensible approach is to combine the power of optimization and computational modeling to obtain a logical outcome for parameters that are not measurable through experimental data collection.

The accuracy and efficacy of any modeling approach depends on the number of variables and level of details considered in the modeling. Body segments' anthropometry, muscle forces and

geometry, bone geometry, material properties of bones and soft tissues, number of segments, reaction forces and so many other parameters are all examples of variables that can either be modeled or simplified in a modeling approach [33], [34]. The complexity of each model has a direct impact on the computational cost and effort required to simulate the model. The trade-off between cost and simplifications of the model is directly affected by the use of each model.

2.3.1 Ground reaction force

Ground reaction force acts between the foot and ground surface. In biomechanical modeling of walking, this ground reaction force can be modeled based on the kinematic constraints [35] or a series of springs and dampers between the foot and ground [18]. The kinematic constraints are based on the COM state and have higher computational cost compared to the second method. Foot-ground interaction force has been modeled using a series of micro spring-damper systems, which their reaction force, has an exponential relation with the distance between foot and ground (Appendix A). Using an exponential function to model the spring force allows us to model a spring force that comes into effect smoothly. The force also diminishes when the distance between the foot and ground becomes sufficiently large. The equation used to model spring-damper forces can be written as follows [36]:

$$F_{y,i} = Ae^{-1150(p_{y,i}-y_0)} - 100v_{y,i}g(p_{y,i}) \quad \text{(Eq. 2.1)}$$

$$g(p_{y,i}) = \frac{1}{1+10e^{500(p_{y,i}-g_0)}} \quad \text{(Eq. 2.2)}$$

Where $v_{y,i}$ is the vertical velocity of the point of application; A is the constant that is dependent on the number of springs used; $p_{y,i}$ is the vertical position of the point of application with respect to the ground surface; y_0 (0.0065905 m) is the parameter that determine when the magnitude of the spring force becomes significant (> 0.5 n); $g(p_{y,i})$ is the element that gradually brings damping in to effect as the foot gets closer to the ground surface and g_0 (= 0.02 m) is the parameter that determines at which point damping starts.

The number of these spring-damper microsystems under each foot is dependent on the computational cost that we are willing to pay and the accuracy that we demand.

2.3.2 Joint moments and muscle excitation

In biomechanical modeling of walking, it is usually preferred to model the *effects* of muscles rather than the muscles themselves [36]. The reason is that for gait, which is a complex motion and many muscles are functioning at the same time, the movements and moments acting on the joints are rather more informative than the forces created by each muscle separately [37]. To this extent, each joint in biomechanical models is actuated by an actuator that accounts for the forces and moments created by the muscles in contact with that specific joint [38]. The force producing characteristics of each actuator depends on the isometric strength of the muscle (F_0^m), fiber length of the muscle (l_0^m), its corresponding pennation angle (α), maximum shortening velocity of the muscle (v_{max}^m) and the rest length of tendon (l_s^T) [37]. Muscles cannot be activated or relaxed instantaneously, thus, the behaviour of muscle activation is proposed to be modeled using a first order differential equation [36].

$$\dot{a} = \left(\frac{1}{\tau_{rise}}\right)(u^2 - ua) + \left(\frac{1}{\tau_{fall}}\right)(u - 1) \quad \text{(Eq. 2.3)}$$

$$-1 < u = u(t) < 1; -1 < a = a(t) < 1 \quad \text{(Eq. 2.4)}$$

Where, $\dot{a}$ is the muscle activation and u is the muscle excitation history. Parameters τ_{rise} and τ_{fall} are the rise and decay time constants of muscle activation and their values are dependent on the joint, muscle characteristics and the task that is being performed.

2.3.3 Forward dynamics

In forward dynamics solution of a biomechanical model, differential equations of motion are numerically integrated forward at every time instant in the simulation. It is a 'forward dynamics' in a sense that forces and moments produce motion and it is distinct from the 'inverse dynamics' where motions are translated into internal forces and moments. Forward dynamics modeling of human gait has been more popular in the past decades [39], [40] because of the advancement in

the development of novel and powerful computational methods and the enhancement of computers that enables consecutive numerical integration of equations of motion on numerous degrees of freedom and dimensions. However, in forward dynamic solutions, all the details and constraints on the model should be accounted for to obtain reasonable and accurate results from the simulations.

2.3.4 Body segments anthropometry

Anthropometric measurements include the body segments' mass (M), inertia (I), length (L), the center of mass location (CG), the range of motion (ROM), and geometry. This information is required to solve the forward dynamics of the system. Anthropometric data are usually obtained from measurements on cadaver [41]. Another benefit of having the anthropometric data is that the results of simulation and modeling can be normalized to body characteristics of the model and a generalized result will be obtained rather than an individual-specific one. In this study, we obtained our anthropometric data based on a 1.8 meters long and 80 kg weighted person [29].

2.3.5 Perturbation modeling

Perturbations acting on the human body during daily activities can be in the form of mechanical perturbations or sensory (e.g. visual) perturbations [42]. The point of application of mechanical perturbations and their dominant frequency and amplitude are effective factors for gait stability. Currently, there is not enough knowledge about the effects of perturbation frequency and amplitude over the stability limits, but it has been proven that the perturbation type and characteristics have a direct impact on the balance of the gait. In this study, we are considering the perturbations acting solely on the BOS of the model in the sagittal plane. The reason for such decision is that movements in the sagittal plane are more dominant on balance control and the perturbations during daily life walking are mostly acting on the BOS of individuals [43].

2.4 Biomechanical mechanism of balanced gait and fall initiation

There are several definitions of balance and stability in the literature. It is commonly believed that "balance is a generic term describing the dynamics of body posture to prevent falling" [29]. Stability defines the state of balance and is a critical aspect for motor control for standing and walking balance, and it is characterized by the motion state of the dynamical system [44]. This motion state can be a multi-dimensional movement trajectory at every time instant, e.g., a combination of COM position and COM velocity as a function of time. The body COM state is stable if small disturbances are attenuated by the dynamical system towards a predefined reference point or trajectory of the COM [45]. For standing balance, the COM state is stable if small disturbances are diminished towards maintaining the upright standing posture. Similar to standing stability, dynamic stability of walking can be achieved if the trajectory of the COM state stays close to the reference trajectory in every time instant of every gait cycle [46]. As such, standing or walking balance requires a combination of COM states, with respect to the BOS, to be within a feasible stability region (FSR) to prevent the loss-of-balance. Otherwise, the loss-of-balance is inevitable, and there is a need for an action for recovery of balance [15]. In the following, we will discuss various approaches to obtain the FSR.

2.4.1 Loss-of-balance and incidence of falling

There is a significant difference between loss-of-balance and incidence of falling [47]. Falls usually occur after loss-of-balance, but not every loss-of-balance leads to an incidence of falling. In fact, in most cases, falls after a loss-of-balance can be prevented by performing an action for recovery [48]. A common action for recovery is taking a further step. In the case of forward locomotion, taking a step forward will help to prevent loss-of-balance. The width of the recovery step depends on the severity of the loss-of-balance state. It is also worth mentioning that loss-of-balance in many cases can assist individuals in their movements. Running can be described as a continuous forward loss-of-balance that requires the human body to take faster steps.

2.4.2 COM states and loss-of-balance

Traditionally, it was believed that for standing and walking balance, the projection of body COM position on the BOS should be within the BOS range at every instant [29]. It was later proved that a combination of position and velocity of body COM (with respect to the BOS) could be indicative of stability state of the body [49]. In 2005, Hof et al. showed that a combination COM position and weighted COM velocity (referred to as 'extrapolated centre of mass (XCOM)') should lie within the boundaries of BOS to maintain stable standing [49]. If the XCOM is outside the BOS range, loss-of-balance occurs. They used the inverted pendulum model as an indicator of the human body during dynamic stance [15]. Later in 2007, Hof et al. expanded his theory to walking and introduced the same biomechanical measure for walking balance [22]. In the following section, we will describe a more inclusive approach to characterize the loss-of-balance.

2.5 Feasible Stability Region (FSR)

The concept of FSR was first introduced by Pai et al. in 1997 [8] FSR is the region inside the state space of body COM states, in which the human body maintains a stable posture without loss-of-balance. If the COM states goes outside the FSR, the loss-of-balance occurs, and further actions for recovery are required to prevent falling [50]. The concept of FSR has been utilized by researchers as a functional approach towards balance assessment [16], [51].

Pai et al. initially introduced a two-segment model for prediction of balance control in the sagittal plane. The proposed model included the whole body pinned to the feet by a revolute joint. The Base of Support (BOS) was the area under the feet [9]. They used an optimization routine to find the maximum and minimum feasible values for the COM velocity for a series of pre-determined COM positions. They obtained a region in the phase diagram of COM motion states (normalized to physiological characteristics of the human body) in which standing balance was feasible. In 2000, Iqbal and Pai et al. introduced a new four-segment model for prediction of standing balance control [14]. They determined the maximum and minimum values for the COM feasible velocities for each initial COM position using a dynamic optimization, for movement termination over the

BOS. In 2008, Yang et al. introduced a seven-segment biomechanical model of the human body in the sagittal plane to analyze walking balance at the toe-off instant [21]. This model was more complex and detailed compared to previously developed models. They utilized an optimization-based simulation towards finding the FSR for walking balance in slip and non-slip conditions (Figure 1).

Several complex, biomechanical models have been developed to simulate gait. Pandy and Anderson developed various three-dimensional (3D) multi-segment models to simulate the human body and muscle forces during the walking and jumping processes [36], [37], [52]. Notably, the computational cost increases with the models complexity, and thus a trade-off for simplicity of the modeling approach used for practical application is inevitable.

2.6 Measurement of COM and BOS using motion capture system

Capturing the trajectory of body COM and BOS using motion-capture cameras and reflective markers is one the most common approaches towards experimental data collection in both clinical and biomechanical research settings [53]. 3D trajectory, rotation, and velocity of a body segment can be determined using a cluster of three or more markers attached to the specified segment. The placement of markers or clusters is specified based on the task and anatomical landmark locations. Marker trajectory measurements are with respect to a predefined global frame, and the recorded position and velocity data are in the same frame. To transform the data into an arbitrary frame, the rotation matrices between the global frame and the arbitrary frame should be calculated.

2.6.1 Global and local Coordinate systems

The global frame of a motion-capture system installed in a lab is defined through a calibration process. Any arbitrary (body-fixed) frame in the 3D space is a local frame with respect to the lab-fixed global frame. Coordinates of markers are recorded in the global frame and can be expressed in any local frame using coordinate transformation [54], [55]. Having the transformation matrix between the local and global coordinate system allows us to interpret any point in 3D space in both

reference frames. The transformation matrix that maps the local frame on the global frame can be written as:

$$ {}^{global}_{local}R = [\vec{X}_l, \vec{Y}_l, \vec{Z}_l] = \begin{bmatrix} \vec{X}_g.\vec{X}_l & \vec{X}_g.\vec{Y}_l & \vec{X}_g.\vec{Z}_l \\ \vec{Y}_g.\vec{X}_l & \vec{Y}_g.\vec{Y}_l & \vec{Y}_g.\vec{Z}_l \\ \vec{Z}_g.\vec{X}_l & \vec{Z}_g.\vec{Y}_l & \vec{Z}_g.\vec{Z}_l \end{bmatrix} = \begin{bmatrix} \cos\theta_{\vec{X}_g\vec{X}_l} & \cos\theta_{\vec{X}_g\vec{Y}_l} & \cos\theta_{\vec{X}_g\vec{Z}_l} \\ \cos\theta_{\vec{Y}_g\vec{X}_l} & \cos\theta_{\vec{Y}_g\vec{Y}_l} & \cos\theta_{\vec{Y}_g\vec{Z}_l} \\ \cos\theta_{\vec{Z}_g\vec{X}_l} & \cos\theta_{\vec{Z}_g\vec{Y}_l} & \cos\theta_{\vec{Z}_g\vec{Z}_l} \end{bmatrix} \quad \text{(Eq. 2.5)} $$

Where each column of the transformation matrix is the projection of a local frame's axis ($\vec{X}_l$, $\vec{Y}_l$, or $\vec{Z}_l$) on the corresponding a global frame's axis ($\vec{X}_g$, $\vec{Y}_g$, or $\vec{Z}_g$). Indices g and l stand for global and local frames, respectively. ɵ is the angle between each of the two axes which their dot product is being calculated. The relation between the coordinates of a specific point (P) in the two frames can be expressed as:

$$ \vec{P}_g = {}^{global}_{local}R.\vec{P}_l + \vec{O}_l \quad \text{(Eq. 2.6)} $$

where $\vec{P}_l$ and $\vec{P}_g$ are the position vectors in the local and global coordinate frames, respectively, $\vec{O}_l$ the position vector of the local frame's origin with respect to the global frame, and ${}^{global}_{local}R$ is the rotation matrix that describes the segment orientation (local frame) with respect to the global frame (Figure 3) [56].

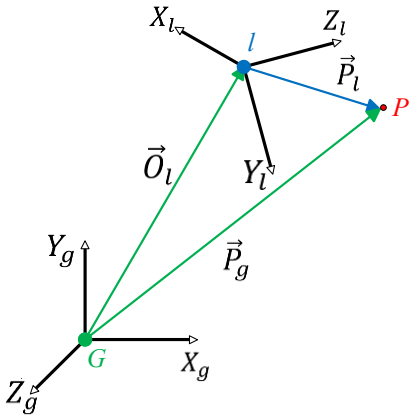

Figure 3: The position of an arbitrary point (P) in both global and local coordinate frames obtained with Eqs. 2.5 and 2.6.

It is possible to reconstruct the 3D trajectory of any virtual point on a body segment using a cluster of markers (at least three markers). As an example, reconstructing the position and trajectory of the first toe (anterior edge of foot, in Figure 4), is possible without having a marker on it and via having the information of at least three other optical markers on a solid plate attached to the foot.

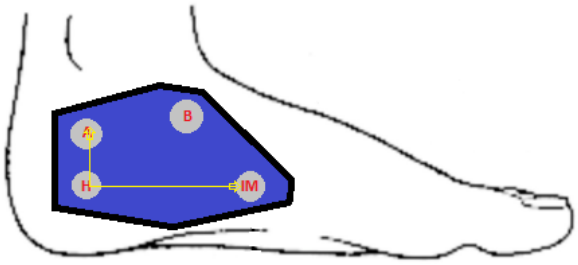

Figure 4: Illustration of the rigid plate attached to the foot along with its optical markers. The virtual toe marker was reconstructed using the orientation and position of the rigid plate and its markers (*A, H,* and *IM*).

$$y_0 = A(t) - H(t),\ Z_0 = IM(t) - H(t),\ X = \frac{(y_0 \times Z_0)}{|y_0 \times Z_0|},\ Y = \frac{(Z_0 \times X_0)}{|Z_0 \times X_0|},\ Z = \frac{(X_0 \times Y_0)}{|X_0 \times Y_0|}$$

$$^{global}_{local}R(t) = [X'\ Y'\ Z'] \qquad \text{(Eq. 2.7)}$$

Where $A(t)$, $H(t)$, and $IM(t)$ are the positions of corresponding markers as a function of time (t) in the global frame for every sample in time. $R(t)$ indicates the orientation of foot plate in the global frame for every sample. For the very first sample, we can reconstruct a virtual toe marker with respect to the markers on the plate using additional information obtained by an auxiliary motion-capture system. This marker is defined to simulate the position and orientation of foot for other time samples. Assuming that the foot is rigid, we can use Eq. 2.8 and find the position of reconstructed toe marker for every time instant using the initial toe marker position instantaneously recorded 3D trajectory the markers on the plate. We can find the BOS kinematics for all time instants, with having the position of the virtual toe marker and heel marker (H) for all time instants.

$$Toe_L\ (t) = Toe_L\ (0) = {}^{global}_{local}R(0))^{-1} * (Toe_G(0) - H_G(0)) \qquad \text{(Eq. 2.8)}$$

$$Toe_G\ (\mathrm{t}) = H_G(\mathrm{t}) + {}^{global}_{local}R(t) * Toe_L(t))$$

Where indices *0*, *G* and *L* indicate initial time, global and local frame, respectively. Reconstructing or finding the position of any other anatomical landmark (i.e. COM) is possible using the same approach. As an example, we found the position of body COM using four markers attached to a plate over the sacrum by averaging their position and translating the averaged value by a margin inside the body for better approximation [57].

2.7 Stability measures

Most of the times stability of a person or a dynamic model arises from its intrinsic properties and movement patterns [9]. The ability to recover from external perturbations and the profile of external perturbation itself are the two factors that govern the probability of falling. Stability measures can reflect that ability of one person to recover from external perturbations whereas these perturbations can be small or large.

Stability measures can be derived from both dynamical system theory (hereafter referred to as mathematical measures) and biomechanical characteristics (hereafter referred to as biomechanical measures) of the walker. The reason to introduce measures derived from dynamical theory is that the system is often non-linear and complex and the explicit equation of human locomotion are unknown. Thus numerical methods rather than analytical methods can be useful. Measures such as variability measures [58], and maximum Lyapunov exponent [59], [60] are based on numerical methods, and dynamic theory whereas XCOM based margin of stability [49] is based on biomechanical modeling of the system.

2.7.1 Variability measures

In many dynamical systems, an increase in the variability of the system's behaviour pattern is indicative of chaos in the system [58], [61]. Variability measures' concept can be applied to gait stability; however, it is of paramount importance to consider that increased variability in a complex dynamical system is not always indicative of chaos alone but can also be indicative of deterministic

characteristics of the system [58]. In general, the variability of a complex dynamical system can thrive from two separate sources; deterministic components of the system (multiple degrees of freedom and complexity of motor control system) and prevailing constraints imposed by the surroundings (external disturbances) [62]. It is crucial to keep in mind that there exist no pragmatic method to distinguish between the effects if the two sources. As a result, variability measures are more useful for balance assessment of simple gait trials with low or no external perturbations [63].

Despite the fact that numerous variability measures have been utilized for balance assessment, commonly used variability measures are based upon deviations of the collected data. Variability measures are mostly utilized over time series of meaningful gait parameters such as stride length, swing phase percentage, gait cycle time, etc. Due to the simplicity of the nature of variability measures and their calculation, variability measures possess noticeable popularity among researchers and clinicians [64]. Measures such as coefficient of variation (CV) and median absolute deviation (MAD) have been utilized to characterize the inter-stride variability of gait cycle time (GCT) and swing phase percentage (SPP) during walking trials.

2.7.2 Biomechanical measures

Stability can be defined straightforwardly in simplified mechanical systems. A typical example of such simple mechanical system is the inverted pendulum, which is commonly used as the simplified model of human standing [65]. For the case of simple static models, body COM has to be controlled to stay over the BOS, but for dynamic models where COM velocity is not zero, this simple model needs to be extended to account for both COM and BOS velocity as well as their position.

Biomechanical measures are thus based upon biomechanical modeling of the system and measurement of body COM and BOS motion states, to be able to assess the stability in spite of the existence of large external perturbations. In the following section, we will describe one of the widely accepted biomechanical measures of stability, i.e., the margin of stability [66].

2.7.2.1 Margin of stability (b)

The concept of XCOM, first introduced by Hof et al. [49], was one of the first stability criterions that considered both position and velocity of COM at the same time. Based on this measure, COM is not necessarily required to be within BOS for stable walking but the XCOM must remain within the BOS limits [15]. The XCOM theory was based on an inverted pendulum model of the human body. Although, this inverted pendulum modeling assumption was descriptive but neglected the effect of arms and upper body movements. Hof et al. showed that for stable walking, feet should be positioned posterior and lateral to the XCOM trajectory. Hof et al. also showed that the deviation of COM states due to external disturbances (perturbations) could be compensated for with multiplying the value of XCOM by a constant, and calculated this constant for sagittal and frontal balance control strategies [15].

The calculation of XCOM requires the measurement of foot placement, COM position (P_{COM}), and COM velocity (V_{COM}) [49].

$$XCOM = P_{COM} + \frac{V_{COM}}{\omega_0} \quad \text{(Eq. 2.9)}$$

Where V_{COM} is COM's velocity in sagittal plane and $\omega_0 = \sqrt{\frac{g}{l_e}}$. g is the gravitational acceleration of earth (= 9.81 m s^{-2}) and l_e is the equivalent pendulum length of the participant. The margin of stability will be written as:

$$b = BOS - XCOM \quad \text{(Eq. 2.10)}$$

The most unstable situation within a step duration is when the value of b is minimum. We can also define the time interval which is needed for COM for XCOM to cross BOS boundaries by:

$$b_\tau = \frac{b}{V_{COM}} \quad \text{(Eq. 2.11)}$$

2.7.3 Conjunction of biomechanical and variability measures

The lack of stability measures based on both biomechanical and variability aspects of a system is sensible throughout the literature. Measures that are solely based on either variability or biomechanical aspects of the human locomotion can neglect either external or natural behaviours of the system [9]. In this study we will introduce series of measures built upon biomechanical and variability characteristics of the system.

Chapter 3

3 Predicted threshold against forward and backward loss of balance for perturbed walking

The material presented in this chapter has been submitted as a research paper (*) to the Journal of Biomechanics. The text formatting of this original paper was altered to match the formatting requirements of the University of Alberta.

* Hosein Bahari, Albert H. Vette, Jacqueline S. Hebert, Hossein Rouhani, "Predicted threshold against forward and backward loss of balance for perturbed walking". Submitted to *Journal of Biomechanics*

3.1 Abstract

The biomechanical mechanisms of loss of balance have been studied during walking with slip and no-slip conditions; but have not been investigated for other perturbation conditions. This study aimed to determine the thresholds of center of mass (COM) velocity and position relative to the base of support (BOS) that predict forward and backward loss of balance during walking with a range of BOS perturbations. BOS perturbations were modeled as sinusoidal BOS motions in the vertical direction or as sagittal rotation. The human body was modeled using a seven-link bipedal model. Forward dynamics alongside with dynamic optimization were used to find the thresholds of initial COM velocity for each initial COM position that would predict forward or backward loss of balance. The effects of perturbation frequency and amplitude on these thresholds were modeled based on the simulation data. Experimental data were collected from 15 able-bodied individuals and 3 individuals with disability during perturbed walking. The simulation results showed similarity with the feasible stability region reported for slip and non-slip conditions. The feasible

stability region shrank when the perturbation frequency and amplitude increased, especially for larger initial COM velocities. 89.5% (71.4%) and 83.0% (68.7%) of the measured COM position and velocity combinations during low (high) perturbations were located inside the simulated limits of the stability region, for non-disabled and disabled individuals, respectively. In summary, the simulation results demonstrated the effects of different perturbation levels on the stability region. The obtained stability region can be used for developing rehabilitative programs in interactive environments.

Keywords: Dynamic optimization; Fall prevention; Forward dynamics; Musculoskeletal modeling; Walking stability.

3.2 Introduction

Falls initiated by loss of balance during gait account for a significant portion of hip fractures and traumatic injuries in older individuals [67], [68]. At least 10 to 20 % of falls lead to injuries that require medical attention [69]. Falls also contribute to self-imposed restrictions of daily activities among the elderly [70] due to subsequent fear of falling. Understanding mechanisms of falling and reasons behind fall initiation can help prevent consequences of falls by developing preventive strategies that can help individuals to maintain balance.

A majority of falls occur during locomotion, such as gait [6]. Human gait stability and its correlation with the variability of gait parameters have long been studied [9][17]. Mathematical tools such as the maximum Lyapunov exponent [11], maximum Floquet multiplier [10], Poincare mapping [12], and standard deviation of step length [13] have been employed to determine the variability in gait parameters and correlate this variability with fall risk. These approaches generally assume that increased variability in walking patterns indicates impaired stability [9]. However, the extent to which these mathematical measures are reliable for perturbed walking circumstances is a matter of debate [9], [20].

Biomechanical mechanisms of walking stability can also be characterized by the state of center of mass (COM) motion (i.e., its position and velocity) with respect to its base of support (BOS) [49].

Various efforts have been taken to develop biomechanical models to quantify dynamic stability during walking [16], [17], [71]. Concepts such as the extrapolated COM [15] and feasible stability region (FSR) [16], [50] were introduced to identify possible combinations of COM motion states for which an individual can maintain balance during a gait cycle. In general, if the COM motion states during walking are within the FSR, loss of balance is not likely to occur. If these states lie below the lower limit of FSR or above the higher limit of FSR, backward loss of balance or forward loss of balance, respectively, is most probable to happen [72].

Previously, the FSR for assessing the dynamic stability of standing and walking in the anterior-posterior direction has been defined using one-link [73], two-link [7], five-link [74], and twelve-link models [75]. While all these models were utilized to find the same FSR in the sagittal plane, the results varied as a function of the number of links [21]; nevertheless, general agreement with the experimental data was found. In addition, FSR during gait followed by a slip was studied using a seven-segment model and a complex optimization routine (Figure 5) that incorporated the physiological, geometrical, and biomechanical limits during walking [21]. However, since only 5% of real-world falls of the elderly occur due to slipping [6], it is valuable to identify the FSR for other walking perturbation conditions.

The modalities of walking perturbation that may cause falling are numerous. Therefore, it is challenging to characterize FSR for every modality of walking perturbation, separately. To develop a model for walking stability and FSR during a wide range of walking perturbations, we propose to model walking perturbations using a combination of sinusoidal motions of the BOS in the three anatomical planes. We hypothesized that obtaining FSR as a function of amplitude and frequency of these sinusoidal motions of the BOS can characterize the FSR for any complex BOS motion. In this study, we only focused on BOS perturbations in the vertical direction and on its rotation in the sagittal plane, and we suggest characterizing the FSR for other modalities of BOS perturbation in the future studies. Our primary objective was to find the effect of external perturbations, modeled using sinusoidal BOS motion, on FSR and, thus, to offer a framework to evaluate the dynamic stability of perturbed walking in the sagittal plane due to complex BOS motions. Our secondary objective was to validate the obtained FSR using experimental data from perturbed walking in a Computer-Assisted Rehabilitation ENvironment (CAREN).

3.3 Methods

3.3.1 Modeling of loss of balance during perturbed walking

A seven-segment bipedal model of the human body in the sagittal plane, based on a previously developed model by Yang et al. [21], was built in Simulink (Mathworks, USA). The model aimed to reconstruct a swing phase of gait, with the right foot acting as the stationary foot. This model consisted of right and left feet, shanks and thighs, along with a head-arms-trunk (HAT) segment (Figure 6.a). Human body was modeled as a seven-segment biomechanical model to account for the movements of lower limbs (feet, shanks, and thighs) in particular. Motion of upper limbs in sagittal plane was less important for us, thus the upper limbs were modeled as one segment (Head-Arm-Trunk segment) leading to a seven-segment model overall. Inputs to the model included initial angle and angular velocity of each joint (θ, $\dot{\theta}$), along with their muscle excitation history in sagittal plane (Eqs. 3.1 and 3.2). The foot-ground reaction force was calculated based on the contact force model presented by previous studies [76]. Inertial characteristics of each body segment were derived based on the literature [29], [41]. In Figure 6, the planar motion of the right foot was reduced to a revolute motion around the anterior edge of foot (right toe) to reconstruct a non-slip situation. The physiological range of motion was used as a constraint for each joint's motion. The model was built based on an 80 kg weighted and 1.8 m tall person's anthropometric data adapted from literature [29]. Similar to [21], [76], physiologically-relevant time-series of joint moments were based on maximum flexion and extension moments and respective equations presented in the literature [17], [77]:

$$\tau = \begin{cases} a(t)T^E & a(t) \geq 0 \\ a(t)T^I & a(t) < 0 \end{cases} \qquad \text{(Eq. 3.1)}$$

$$\dot{a} = \frac{u-a}{t_{activation}}, \qquad -1 \leq u(t), a(t) \leq 1 \qquad \text{(Eq. 3.2)}$$

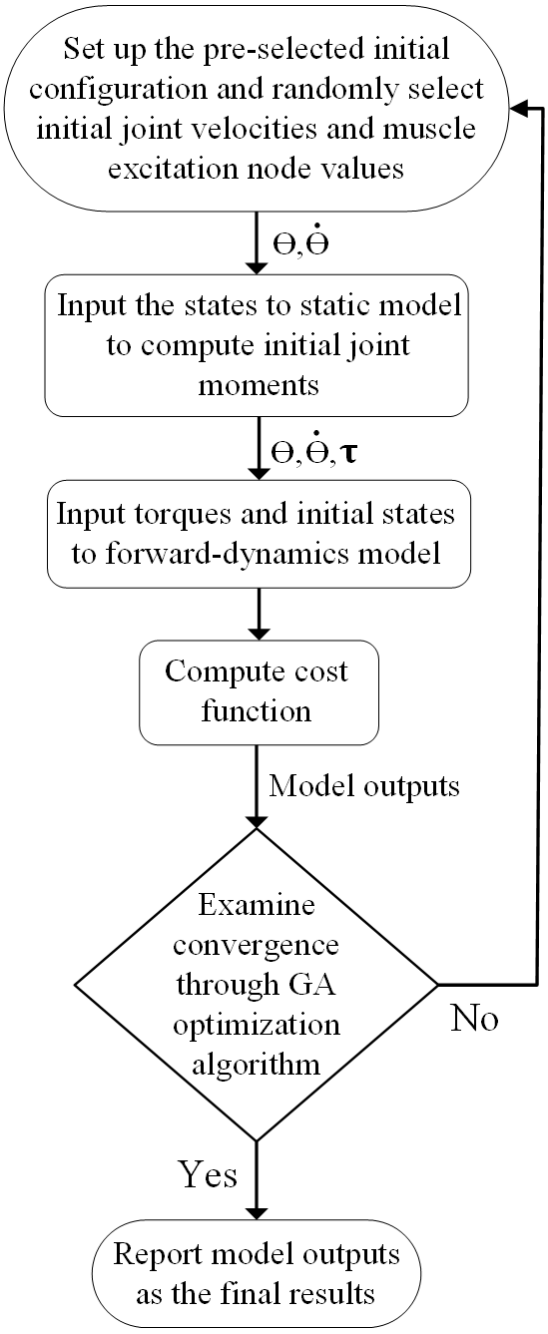

Figure 5: Flowchart of simulation and optimization process: An initial model was used to determine the initial joint moments at the instance of foot toe-off. Inputs to this model were each joint's initial angle obtained from experimental data. Then, a forward dynamics model was used to perform movement simulation. Inputs to this model were each joint's initial angle, angular velocity, torque, and muscle excitation history.

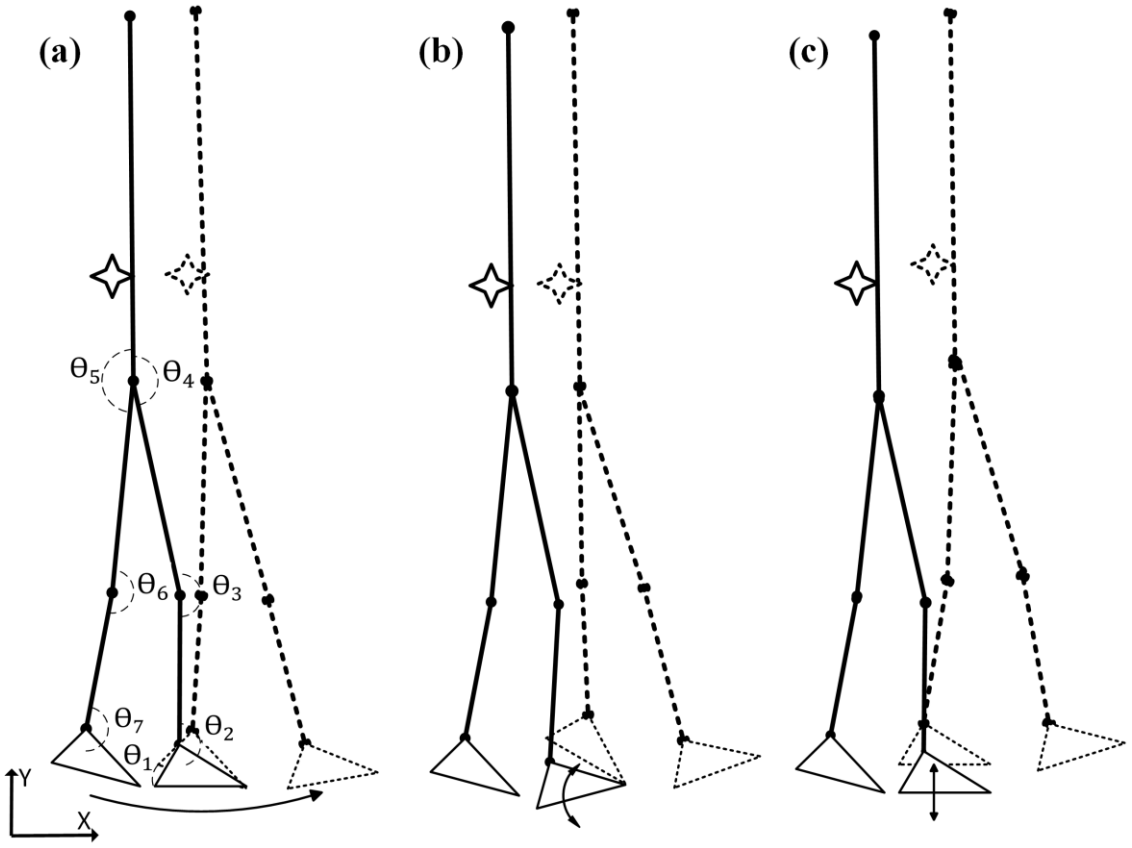

Figure 6: (a) schematic of the bipedal human model in the sagittal plane. The model parameters were defined by a group of joint angles $(\theta_1, \theta_2, \dots, \theta_7)$. (b) and (c) show the base of support (BOS) perturbation as a rotation in the sagittal plane and as a vertical displacement, respectively.

A Genetic Algorithm (GA) optimization method was used to find the thresholds against backward and forward loss of balance (Figure 5). The input to the optimization routine included 76 control node values, seven initial angular velocities, and seven initial angles corresponding to the body joints. The optimization routine was solved for six cases of vertical perturbation, six cases of sagittal rotation perturbation, and one case of unperturbed walking (Figure 6.b and 6.c). Two separate optimization cost functions (CF) were used to find the maximum and minimum feasible initial velocities to prevent forward and backward loss of balance. The cost function to find the minimum initial velocity of the COM was chosen based on previous studies [21], including a few

enhancements to model a smooth and more natural progression of swing phase, necessary for analyzing the stability of perturbed walking:

$$CF_{backward} = w_1\,\dot{x}_{COM}^{initial} + w_2\left|\dot{x}_{COM}^{final}\right| + w_3\int_{t_i}^{t_f} e\big(F_y(t)\big)dt + w_4\int_{t_i}^{t_f} e(\Theta(t))dt + w_5\int_{t_i}^{t_f} e\big(\dot{\Theta}(t)\big)dt + w_6\int_{t_i}^{t_f}\left\lfloor \min\big(y_{l,toe}(t), y_{l,heel}(t)\big)\right\rfloor dt + w_7 e\big(x_{COM}^{final} - x_{r,heel}^{final}\big) + w_8\int_{t_i}^{t_f}\tau(t)^2 dt + w_9\left\lfloor x_{l,heel}^{final} - x_{r,toe}^{final}\right\rfloor + w_{10}\left|y_{HAT\ COM}^{initial} - y_{HAT\ COM}^{final}\right| + w_{11}\int_{t_i}^{t_f} e\big(y_{l,heel} - y_{r,heel}\big)\,dt + w_{12}\sum_{i=1}^{6}\int_{t_i}^{t_f} SD(\Theta_i)\,dt \qquad \text{(Eq. 3.3)}$$

In Eq. (3.3), integrals were taken over the simulation time to ensure that no physiological constraint is violated during the simulation. Subscripts *r* and *l* indicate right and left foot, and t_i , t_f indicate the initial and final time instance of the simulation, respectively. The $e(x(t))$ and $\lfloor x(t) \rfloor$ functions are defined in [21]. The rationale for including the first to eighth terms in the cost function has been discussed in [21]. However, we added terms 9, 10, 11, and 12 to the previously developed cost function. The ninth term ensures the left foot is placed in front of the right foot at the end of simulation and a complete swing phase is performed. The tenth term ensures the HAT segment remains upright and almost at constant height with physiologically meaningful motions. The eleventh term guarantees the left heel is in contact with the ground at the end of simulation. Finally, the twelfth term ensures each segment's angle changes smoothly and does not illustrate rapid movements (SD: standard deviation). Adding these terms is important for perturbation analyses where relative motion of body segments is important compared to the unperturbed case where the support surface is motionless. These terms particularly, assured an almost upright posture of the trunk segment and a smooth leg swing during perturbed gait.

A similar cost function was used to find the maximum initial velocity:

$$CF_{forward} = w_1\,/\dot{x}_{COM}^{initial} + w_2\left|\dot{x}_{COM}^{final}\right| + w_3\int_{t_i}^{t_f} e\big(F_y(t)\big)dt + w_4\int_{t_i}^{t_f} e(\Theta(t))dt + w_5\int_{t_i}^{t_f} e\big(\dot{\Theta}(t)\big)dt + w_6\int_{t_i}^{t_f}\left\lfloor \min\big(y_{l,toe}(t), y_{l,heel}(t)\big)\right\rfloor dt + w_7 e\big(x_{COM}^{final} - x_{r,toe}^{final}\big) + w_8\int_{t_i}^{t_f}\tau(t)^2 dt + w_9\left\lfloor x_{l,heel}^{final} - x_{r,toe}^{final}\right\rfloor +$$

$$w_{10}\left|y_{HAT\ COM}^{initial} - y_{HAT\ COM}^{final}\right| + w_{11}\int_{t_i}^{t_f} e\left(y_{l,heel} - y_{r,heel}\right) dt + w_{12}\sum_{i=1}^{6}\int_{t_i}^{t_f} SD(\Theta_i)\, dt \quad \text{(Eq. 3.4)}$$

The change in the first and seventh term was made to obtain the maximum initial velocity and to end the swing phase with a COM position behind the front end of BOS (right toe), respectively. A trial and error approach was used to determine the optimal weight of each term in both cost functions (w_i). In all simulations, the right foot was assumed to be fxed to the BOS, and the COM motion states were calculated with respect to the BOS. The BOS motion was assumed to be sinusoidal: translational in the vertical direction and, in separate simulations, rotational in the sagittal plane. The amplitude of these sinusoidals was assumed to be ±5 cm, ±10 cm, and ±15 cm for vertical displacemets and ±1.5°, ±5°, and ±10° for sagittal rotations. Their frequency was assumed to be 1 Hz and 3 Hz. These values were chosen based on the perturbation profiles implemented in the experiments conducted in the CAREN (see Section 3.3.2). We then obtained the FSR limits for each amplitude and frequency and for each perturbation modality, as well as for the unperturbed condition. We modeled the FSR limits for backward and forward loss of balance as second-order polynomials:

$$\dot{x}_n = a_1.x_n^2 + a_2.x_n + a_3 \quad \text{(Eq. 3.5)}$$

where $\dot{x}_n$ and x_n are the normalized relative velocity and position of the COM, respectively. Subsequently, we modeled the parameters of these polynomials (a_i) as a function of perturbation amplitude (A) and frequency (f) using a least-square error minimization approach:

$$a_i = b_1.f + b_2.A + b_3.f.A + b_4 \quad \text{(Eq. 3.6)}$$

3.3.2 Experimental validation

To evaluate the obtained FSR limits through simulations in Section 3.3.1, we compared them with those previously presented in the literature. In addition, experimental data for the cases of perturbed and unperturbed walking were collected. Experiments were conducted using a CAREN. Fifteen non-disabled individuals having average body height and body weight of 1.79±0.09 m and 78.7±5.8 kg, respectively, and three individuals with amputation (one with unilateral trans-femoral, one with unilateral trans-tibial, and one with unilateral upper limb amputation and sustained traumatic brain injury) (body height: 1.78±0.1 cm; body weight: 75.7±3.8 kg) participated in this study. The experimental protocol was approved by the local research ethics board (protocol number: Pro00066076), and all participants gave informed consent. Each participant performed a walking trial including four sessions: One session of 30 meters of unperturbed walking, followed by three sessions of 60 meters of perturbed walking. Walking trials were performed on a treadmill, which adapted to the speed of walking of each individual to model their natural walking situation. Perturbations were delivered in the form of random vertical displacements or random sagittal plane rotations of the platform. Perturbations increased in amplitude (ranging from ±0.01 meters to ±0.08 meters in the vertical direction and 0 to ±3 degrees in rotation). The COM position and velocity as well as the BOS position and velocity were calculated using data from optical motion capture (Vicon Inc., Oxford, United Kingdom). The BOS motion was tracked using four markers placed on a rigid plate attached to each foot, whereas COM motion was tracked using four markers placed on a rigid plate attached to a belt around the sacrum. Four additional markers were used to track the motion of the platform. We obtained the COM motion states (with respect to the BOS) and investigated if they were within the FSR obtained through simulations.

3.4 Result

The FSR limit for backward loss of balance obtained in the present study for non-slip, unperturbed walking was more conservative than that reported by Pai et al. [8]who used a two-segment model. Our obtained limit for forward loss of balance was close to that reported by Pai et al.[8]. Our obtained limit for backward loss of balance was, however, less conservative than that obtained by

Yang et al. Note that Yang et al. [78] used the same body model, but implemented a different optimization cost function and also simulated a slip condition (Figure 7).

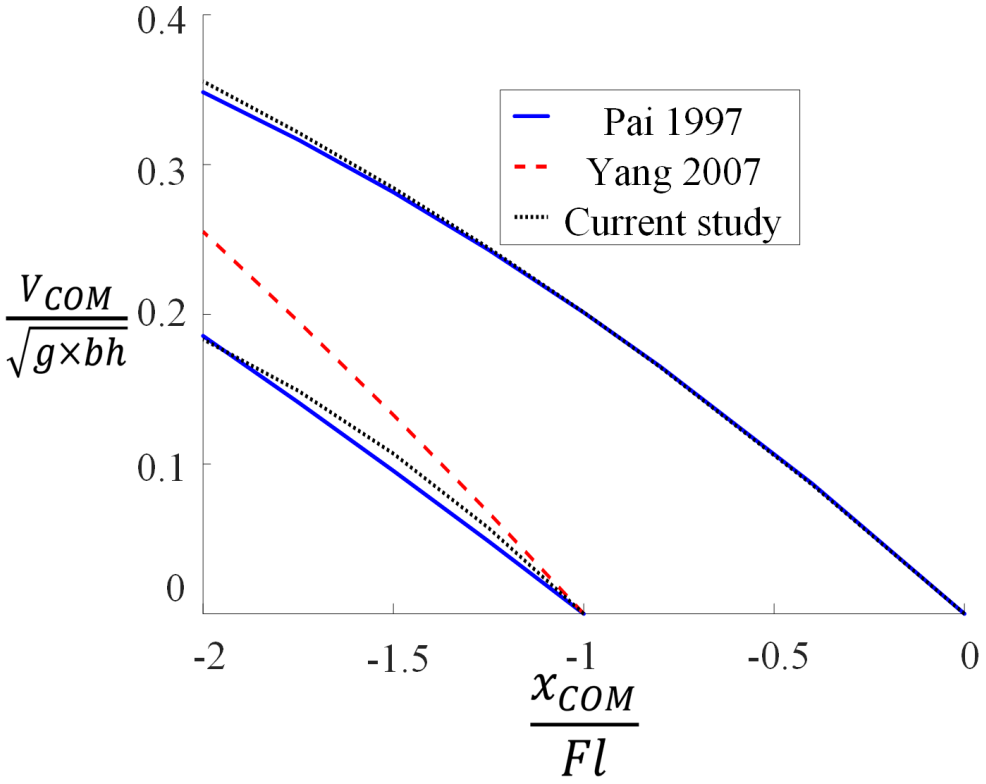

Figure 7: Limits of the feasible stability range (FSR), obtained for backward and forward loss of balance, in the center of mass (COM) motion state space. COM position and velocity (relative to the base of support; BOS) were normalized to foot length (*Fl*) and $\sqrt{g \times bh}$ (*g*: gravitational acceleration; *bh*: body height), respectively. Values of 0 and –1 on the horizontal axis indicate the location of the right toe and heel, respectively. These limits (shown as red lines) are compared to those obtained by Pai et al. [8] and Yang et al. [78] for non-slip conditions that used a different number of segments and/or optimization cost function.

According to Figure 8, an increase in both the amplitude and frequency of the vertical displacement and sagittal rotation resulted in a reduced range of FSR for both backward and forward loss of balance. Table 1 presents the limits of backward and forward loss of balance, modeled as second-order polynomials for different amplitudes and frequencies of the vertical displacement and

sagittal rotation of the BOS. The limit of forward loss of balance could be modeled as a line, since the coefficients of the second-order term were close to zero. Using the results presented in Table 1, each of the second-order polynomial parameters (a_i) was modeled as a function of perturbation frequency and amplitude, as illustrated in Table 2.

Table 1: Limits of backward and forward loss of balance during walking with vertical displacement and sagittal rotation perturbations of the base of support (BOS). Each type of perturbation is modeled as a sinusoidal motion with different levels of frequency (*f*) and amplitude (A). For each perturbation condition, the first and second rows indicate a polynomial equation that models the limits of backward and forward loss of balance, respectively. These equations are expressed in the form of $\dot{x}_n = a_1.x_n^2 + a_2.x_n + a_3$, $\dot{x}_n.\ x_n$ stand for COM velocity and position, with respect to the BOS, and normalized to $\sqrt{g \times bh}$ (g: gravitational acceleration; bh: body height) and foot length, respectively.

Vertical displacement	**Polynomial**
***f*= 1 Hz**	$\dot{x}_n = -0.026\,x_n^2 - 0.274\,x_n - 0.244$
A= ±5 cm	$\dot{x}_n = -0.036\,x_n^2 - 0.243\,x_n$
***f*= 1 Hz**	$\dot{x}_n = -0.041\,x_n^2 - 0.324\,x_n - 0.283$
A= ±10 cm	$\dot{x}_n = -0.009\,x_n^2 - 0.194\,x_n$
***f*= 1 Hz**	$\dot{x}_n = -0.122\,x_n^2 - 0.582\,x_n - 0.459$
A= ±15 cm	$\dot{x}_n = 0.001\,x_n^2 - 0.172\,x_n$
***f*= 3 Hz**	$\dot{x}_n = -0.082\,x_n^2 - 0.443\,x_n - 0.361$
A= ±5cm	$\dot{x}_n = -0.041\,x_n^2 - 0.243\,x_n$
***f*= 3 Hz**	$\dot{x}_n = -0.080\,x_n^2 - 0.457\,x_n - 0.376$
A= ±10 cm	$\dot{x}_n = -0.026\,x_n^2 - 0.210\,x_n$
***f*= 3 Hz**	$\dot{x}_n = -0.101\,x_n^2 - 0.536\,x_n - 0.436$
A= ±15 cm	$\dot{x}_n = -0.009\,x_n^2 - 0.179\,x_n$

Sagittal rotation	**Polynomial**
***f*= 1 Hz**	$\dot{x}_n = -0.129\,x_n^2 - 0.621x_n - 0.491$
A= ±1.5º	$\dot{x}_n = -0.041\,x_n^2 - 0.263x_n$
***f*= 1 Hz**	$\dot{x}_n = -0.098\,x_n^2 - 0.558x_n - 0.460$
A = ±5º	$\dot{x}_n = -0.042\,x_n^2 - 0.254x_n$
***f*= 1 Hz**	$\dot{x}_n = -0.114\,x_n^2 - 0.610x_n - 0.496$
A= ±10º	$\dot{x}_n = -0.047\,x_n^2 - 0.253x_n$
***f*= 3 Hz**	$\dot{x}_n = -0.152\,x_n^2 - 0.670x_n - 0.548$
A= ±1.5º	$\dot{x}_n = -0.050\,x_n^2 - 0.266x_n$
***f*= 3 Hz**	$\dot{x}_n = -0.101\,x_n^2 - 0.574x_n - 0.473$
A= ±5º	$\dot{x}_n = -0.045\,x_n^2 - 0.247x_n$
***f*= 3 Hz**	$\dot{x}_n = -0.104\,x_n^2 - 0.591x_n - 0.487$
A= ±10º	$\dot{x}_n = -0.053\,x_n^2 - 0.251x_n$

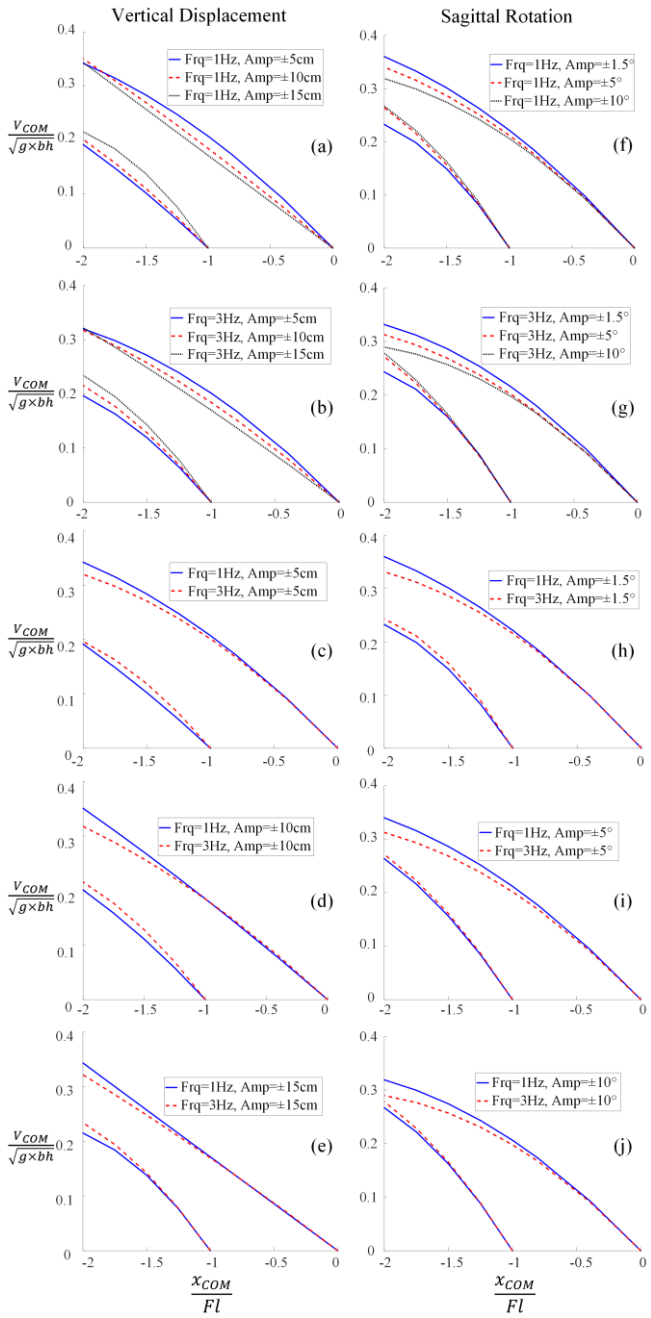

Figure 8: Effects of frequency and amplitude of the perturbations on the limits of the feasible stability range (FSR). Plots (a) to (e) show the FSR limits when base of support (BOS) perturbations are modeled as sinusoidal movements in the vertical direction, and plots (f) to (j) show the FSR limits when BOS perturbations are modeled as a sinusoidal rotation between right foot and the horizontal plane. The center of mass (COM) position and velocity are normalized as in Figure 7.

Table 2: The parameters of the polynomial equations that modeled the limits of backward and forward loss of balance in Table 1, modeled as a function of frequency and amplitude of perturbation. This equation is expressed as $\dot{x}_n = a_1.x_n^2 + a_2.x_n + a_3$ for each perturbation condition. Each parameter (a_i: a_1, a_2, or a_3) is modeled as $a_i = b_1.f + b_2.A + b_3 f.A + b_4$, where f stands for frequency in Hz and A stands for amplitude in meters (vertical displacement perturbation) and radians (sagittal rotation perturbation).

	Vertical displacement	**Sagittal rotation**
a_1 **for upper limit**	$-0.012f + 0.210A + 0.050f.A - 0.027$	$-0.007f - 0.116A + 0.035f.A - 0.027$
a_2 **for upper limit**	$-0.017f + 0.388A + 0.108f.A - 0.232$	$-0.012f - 0.158A + 0.097f.A - 0.235$
a_3 **for upper limit**	0	0
a_1 **for lower limit**	$-0.0011f - 0.285A - 0.039f.A - 0.040$	$-0.027f - 0.289A + 0.213f.A - 0.073$
a_2 **for lower limit**	$-0.003f - 0.998A - 0.188f.A - 0.304$	$-0.090f - 1.320A + 0.676f.A - 0.419$
a_3 **for lower limit**	$-0.001f - 0.705A - 0.158f.A - 0263$	$-0.073f - 1.050A + 0.526f.A - 0.342$

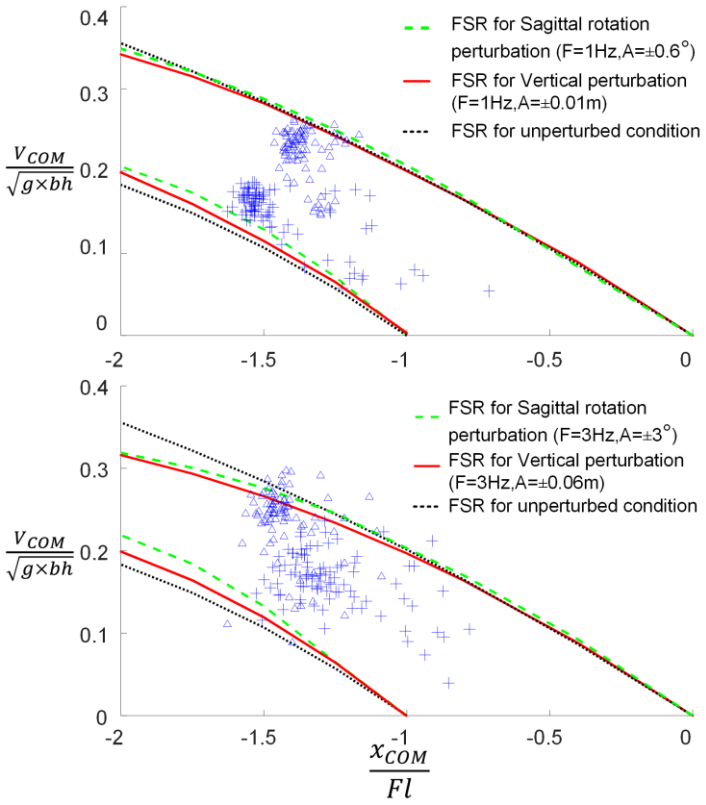

Figure 9: COM position and velocity obtained experimentally for two walking trials of one representative non-disabled participant (+ points) and one case of participant (Δ points) with amputation (feasible stability limits, FSR, obtained through simulation results). + and Δ Points illustrate right foot lift-off instances. The top graph is representative of the walking trial with low perturbation intensity (vertical displacements and sagittal rotations with frequency of 1 Hz and amplitudes of ±1cm and ±0.6º, respectively), and the bottom graph is representative of the walking trial with high perturbation intensity (vertical displacements and sagittal rotations with frequency of 3 Hz and amplitudes of ±6 cm and ±3º, respectively).

For each walking perturbation condition, a majority of the experimentally obtained COM motion states of non-disabled individuals and individuals with amputation were within the FSR obtained through simulation (Figure 9). In trials with the higher perturbation level, we observed more scattered COM motion states for both initiation and termination of a swing phase.

For non-disabled participants, an average of 89.5% of experimentally recorded COM motion states at the toe-off instance were initiated inside the FSR limits for both vertical displacement and

sagittal rotation conditions (120 to 200 steps) under the low perturbation condition (frequency of 1 Hz and amplitudes of ±1 cm and ±0.6º). For the high perturbation condition (frequency of 3 Hz and amplitudes of ±6 cm and ±3º), the mentioned ratio was 71.4%. For participants with amputation, these ratios were 83.0% and 68.7% for low perturbation and high perturbation conditions, respectively. The FSR limits for high and low perturbation conditions were obtained using the coefficients presented in Table 2. Reported values contain both right and left toe-off instances of each participant during perturbed treadmill walking trials. The number of steps and toe-off instances varied among participants due to the fact that the walking trials were designed for a fixed walking distance, rather than a fixed number of steps as well the loss of camera recording for a number of gait cycles.

3.5 Discussion

The human body faces a variety of walking perturbation modalities during daily life. To reduce the risk of falling due to real-world perturbations, rehabilitation programs in virtual reality environments such as the CAREN have been developed. Similar to real-world perturbations, these environments can apply walking perturbations using complex motions of a moving platform. A prerequisite for developing individual-specific, efficient rehabilitation programs is to quantify the dynamic stability and risk of loss of balance during perturbed walking, as a function of the perturbation profile. Although the FSR for unperturbed walking and a few perturbation conditions (e.g., slip) have been reported in the literature [21], [79], there is currently no model for the FSR during complex walking perturbations similar to those applied by the CAREN platform. We assumed that the complex translational and rotational motions of the CAREN platform can be molded as a series of sinusoidal motions in each direction. The original contribution of this study was to determine the FSR limits as a function of the amplitude and frequency of the sinusoidal movements of BOS in the vertical direction and as sagittal rotation. We used a seven-link model of the body previously developed in the literature [21]. However, we modified the previously suggested dynamic optimization and added additional terms to its cost function to ensure smooth and realistic motion of the body during the swing phase, improve the accuracy of the estimated FSR, and enable modeling of loss of balance during perturbed walking. The FSR from our

simulation process for unperturbed walking derived from our proposed optimization cost function and seven-link model was similar to those previously reported by Pai et al. [8] and Yang et al. [21]. Particularly, our study presents a more conservative FSR limit for backward loss of balance compared to the previously reported ones [21], with the same seven-segment model and a similar optimization cost function. Comparing the experimentally recorded COM motion states with the modeled limits of FSR can provide mechanistic insights into the human motor control system under perturbed conditions for individuals with different neuromuscular impairments.

We modeled the upper and lower limits of the FSR as second-order polynomials and obtained the polynomial parameters as a function of the perturbation amplitude and frequency for vertical displacements and sagittal rotations of the BOS. Our results show that an increase in both amplitude and frequency shrinks the FSR boundaries. This suggests that more conservative strategies are required for balance control of COM motion states in the case of perturbed walking.

The collected COM motion sates were experimentally collected for non-disabled individuals as well as for individuals with trans-femoral or trans-tibial amputation or brain injury during walking, with high and low levels of perturbation. A majority of the COM motion states at the beginning of the swing phase (toe-off event) were located within the FSR limits. A number of these COM motion states at the beginning of the swing phase were outside of the FSR range, with no fall occurring. The portion of the COM motion states lying outside the FSR limits increased from 10.5 to 28.6% (for non-disabled individuals) when increasing the perturbation intensity, which is consistent with the increased variability of gait [80] expected with higher levels of perturbation.

Note that the presented FSR limits for backward and forward loss of balance are relative measures and do not deterministically predict the loss of balance and falling. Therefore, similar to previous studies, we expect to observe a number of COM motion states outside the estimated FSR, without an incidence of falling [21] for the following reasons: First, our proposed model predicted only biomechanical mechanisms of loss of balance. The thresholds for loss of balance and falling may change due to psychological or cognitive reasons. Second, our estimation of the physiological ranges of joint moments and the ability of an individual to control them was based on models reported in the literature (Eqs. (3.1) and (3.2)) [27], [31]. The model parameters and the maximum joint moments are expected to change as a function of an individual's neuromuscular condition,

and not considering such variability in our study is a limitation. Third, loss of balance does not usually result in falling, but requires an action for recovery. An individual who is at high risk of loss of balance usually adopts a modified control strategy to maintain their balance in the presence of a perturbation, such as taking recovery steps or changing the step length and width during walking. Fourth, assuming the HAT as a rigid segment neglects the motion of the upper limbs and their potential contribution to walking stability. Although this contribution is reported to not be significant for slip condition [81], it is possible that during applied perturbation in our experiments, the COM motion states moved out of the FSR, but that the upper limbs and trunk motion brought the COM motion states back to the FSR. Fifth, we modeled body movements only in the sagittal plane, whereas perturbations and movements in the frontal plane can alter the limits of FSR. These two latter topics along with the effect of BOS perturbation in anterior-posterior direction on the FSR should be investigated in the future. Despite these limitations and the influence of these balance mechanisms that must be studied in the future, the present study accomplishes the first step for such future studies. Our study also quantified the challenges that individuals with neuromuscular impairment would face in a specific perturbation condition and, thus, contributes to the development of rehabilitative programs.

3.6 Conclusions

This study quantified the effect of walking perturbations in the forms of vertical displacements of the base of support (ground) and its rotation in the sagittal plane on the FSR against backward and forward loss of balance. Considering the limitations of this study, we can support the integrity of our results by relying on the comparison with FSR limits presented in the literature and on our experimental results from non-disabled individuals and individuals with amputation during walking. The FSR limits provided in this study can be used as a basis for developing rehabilitative programs conducted in virtual reality environments such as the CAREN and for providing training guidelines for participants with walking disabilities. The findings of this study can also enhance our mechanistic understanding of human motor control under different walking perturbation conditions.

Chapter 4

4 Extended feasible stability region: An approach to assess stability of perturbed walking

The material presented in this chapter has been submitted as a research paper (*) to the Journal of Biomechanics. The text formatting of this original paper was altered to match the formatting requirements of the University of Alberta.

(*) Hosein Bahari, Juan Forero, Jeremy C. Hall, Jacqueline S. Hebert, Albert H Vette, Hossein Rouhani. “Extended feasible stability region: An approach to assess stability of perturbed walking”. Submitted to Journal of Biomechanics

4.1 Abstract

Walking stability has been assessed through gait variability or biomechanical measures that are usually unable to characterize the instantaneous risk of loss-of-balance as a function of gait parameters, body sway, and physiological and perturbation conditions. This study aimed to introduce and validate biomechanical measures for walking stability as a function of these parameters under various perturbed walking conditions.

We extended the use of the concept of feasible stability region (FSR) and introduced an ‘extended FSR (ExFSR)’ that characterizes walking stability for a full step, and proposed novel stability measures based on the proximity of the body center of mass (COM) position and velocity to the ExFSR limits . We quantified perturbed walking of fifteen non-disabled individuals and three individuals with disability, and calculated inter-stride variability of gait parameters, the extrapolated-COM-based margin of stability, and our proposed ExFSR-based measures.

11.1% (30.8%) and 25.4% (33.3%) of the measured trajectories of the COM position and velocity during low (high) perturbations went outside the calculated extended FSR limits, for non-disabled and disabled individuals, respectively. These measures significantly correlated with the extrapolated-COM-based margin of stability in both perturbation conditions, and with inter-stride variability of swing phase percentage in the high-perturbation condition.

The credibility of the ExFSR-based measures was supported by their experimentally-observed correlation with existing measures. The ExFSR-based measures facilitate our understanding on the biomechanical mechanisms of loss-of-balance as a function of gait parameters, body sway, and physiological and perturbation conditions. As such, these measures can contribute to the development of rehabilitative programs.

Keywords: balance assessment; computational biomechanics; fall prevention; forward dynamics; gait stability.

4.2 Introduction

It has been observed that the risk of falling during daily life increases with aging [82] and chronic neuromuscular disorders [80]. Falls pose a noticeable threat to the growing population of elderly people [68] as they can result in serious physical injuries [69] or psychosocial complications due to self-imposed restrictions caused by fear of falling [70]. Quantifying the risk of falling contributes to designing prevention strategies and, thus, reducing the incidence of falling.

A considerable portion of falls occurs during walking [6]. Stable walking can be defined as "gait that does not lead to falls despite perturbations" [9]. On the one hand, walking stability has been characterized using measures based on dynamic system stability [9], such as maximum Lyapunov exponent [83], long-range correlation [62] and variability measures [58]. They assess the ability of the system to nullify the effects of small external perturbations, but cannot quantitatively separate the effects of walking pattern and external perturbation conditions on the risk of loss-of-balance. On the other hand, walking stability can be characterized using measures derived from biomechanical models. Such measures account for circumstances and conditions governing the

real-world environments. Consequently, the effects of the external perturbations and of physiological and environmental conditions on these biomechanical measures can be characterized [84]. These measures obtain the limits of a feasible stability region (FSR) in which the COM states should lie to maintain dynamic balance during walking [8], [15]. Complex biomechanical models in combination with optimization processes have been proposed to obtain the FSR limits for standing and walking [21], [85].

A common example of human body modeling is the inverted pendulum modeling of standing [8]. Other biomechanical models with more segments and higher complexity have also been developed to account for the effects of several body segments [19], [86]. Despite the potential for modeling the effects of complex perturbation conditions on loss-of-balance, biomechanical stability measures have not been widely employed to investigate loss-of-balance in daily conditions and were not implemented in clinical research, mainly due to their computational and mathematical complexity.

We recently developed a seven-segment bipedal model of human walking (similar to [21]) and developed a methodology to obtain the FSR limits as a function of the amplitude and frequency of complex BOS perturbations in the sagittal plane, and validated it for balance at toe-off [85]. The primary objective of the present study is to define biomechanical stability measures in the sagittal plane based on an extension of the FSR concept for full steps during unperturbed and perturbed walking based on this previously developed model. The secondary objective is to support the credibility of our proposed measures by showing their correlations with other previously reported stability measures using experimental data gathered during perturbed walking in a Computer-Assisted Rehabilitation ENviroment (CAREN). These proposed stability measures will characterize loss-of-balance as a function of the COM motion during walking, gait parameters, and physiological and perturbation conditions.

4.3 Methods

4.3.1 Modeling Loss-of-Balance

To find the FSR in the sagittal plane during an entire step for the cases of unperturbed and perturbed walking, we used a seven-segment bipedal model of a walking human similar to the one in [21] (Figure 10). The model was capable of obtaining the FSR at the toe-off instant of the swing (following) foot where the BOS was the standing (leading) foot in contact with the ground. Although our previously obtained FSR in chapter 3 [85] was introduced and tested for the toe-off instant, experimental data gathered during various walking trials showed that body COM states eventually leave the FSR during the swing phase period. This would not necessarily result in loss-of-balance because the BOS expands to the area under and between both feet as soon as the swing foot touches the ground in front of the standing foot at the beginning of the double-support phase (i.e., heel-strike instant). Then, the COM states would be once again located in the succeeding FSR based on the succeeding BOS location and, thus, both COM and BOS progress during walking.

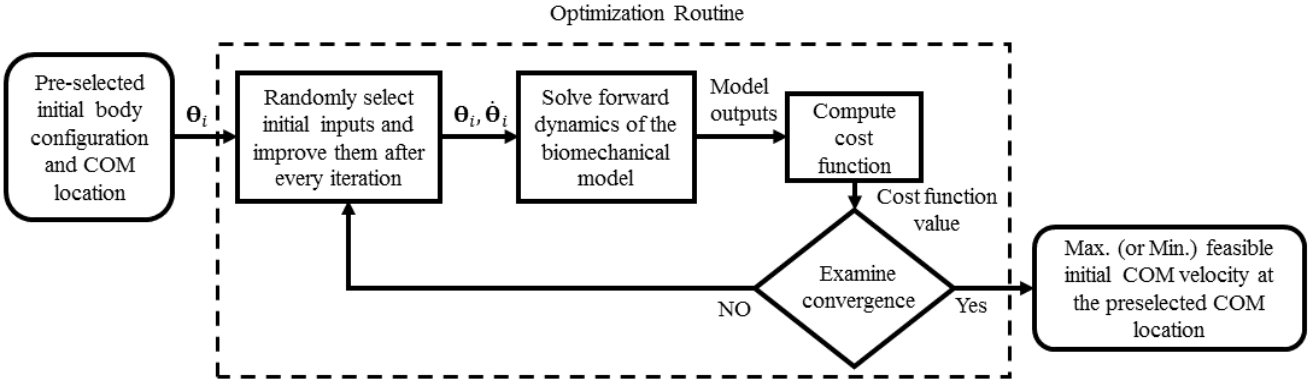

Figure 10: Illustration of optimization and simulation process used to obtain the Feasible Stability Region (FSR) limits for perturbed walking conditions. The output of the optimization process is the maximum and minimum feasible normalized COM velocity for every initial COM position.

Given that each step is composed of a swing phase and a succeeding double-support phase, we assume in the present study that:

i) balance at the beginning of the step (i.e., the toe-off instant of the swinging foot) will not be lost as long as the COM state stays within the FSR pertaining to the standing foot (posterior foot in Figure. 11);
ii) balance at the end of the step (i.e., the toe-off instant of the ex-standing foot) will not be lost as long as the COM state stays within the FSR pertaining to the ex-swinging foot (anterior foot in Figure 11); and
iii) balance during the swing phase and its succeeding double-support phase will not be lost as long as the COM state stays in front of the lower limit of the FSR pertaining to case (i) and behind the upper limit of the FSR pertaining to case (ii).

Therefore, to expand the definition of FSR to assess the stability of consecutive steps, we defined the 'Extended Feasible Stability Region (ExFSR)' for the duration of one step; accordingly, ExFSR consisted of the FSR pertaining to both feet, and the state space between them. Note that these two FSRs are separated by the distance between the posterior foot's anterior edge (toe) and the anterior foot's posterior edge (heel) for the duration of the double-support phase (Figure 11). The distance between the two feet (D) at the heel strike instant was measured using the reflective markers attached to each foot.

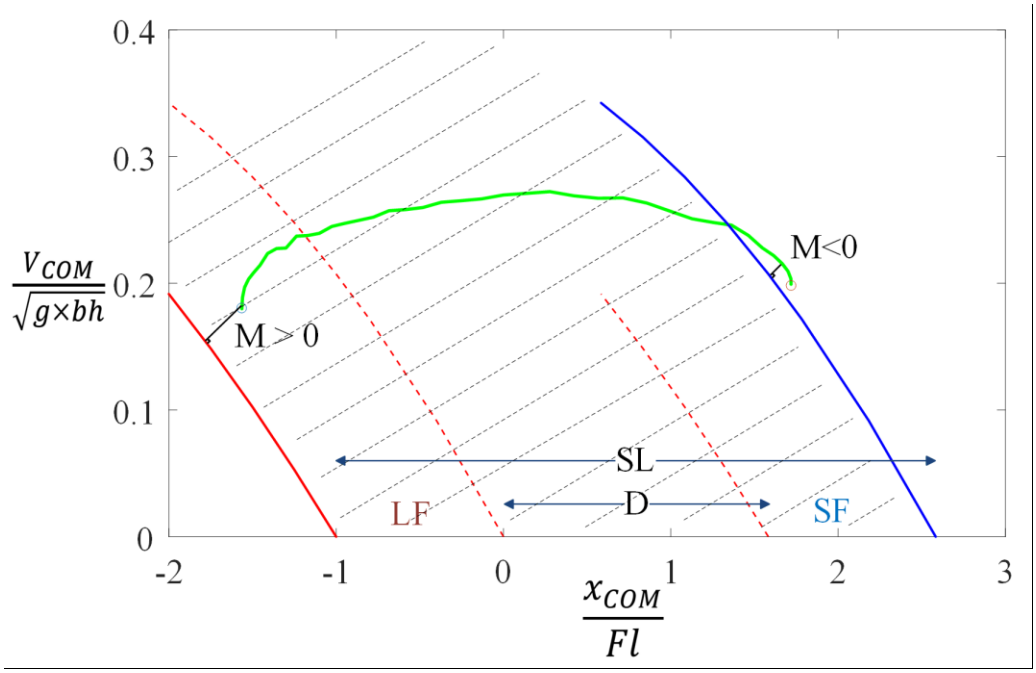

Figure 11: Extended Feasible Stability Region (ExFSR), along with the body's COM motion trajectory for the duration of one foot's toe-off instant to the next foot's toe-off instant (one complete swing phase and the following double-support phase). ExFSR region has been marked with transparent dashed lines. The shortest distance between the COM motion trajectory and the lower and upper limits of ExFSR (M_L(n) and M_U(n)) was measured as the stability measure. LF, SF and SL stand for standing foot, swinging foot, and step length, respectively.

Then, we introduced the shortest distance from the trajectory of the COM state to the lower and upper boundary (limit) of the ExFSR as the 'measure of stability (i.e., *$M_L(n)$ and $M_U(n)$*, respectively)' that characterized the risk of backward and forward loss-of-balance, respectively, during one isolated step during human gait (*n* is the step index). *M(n)* (*i.e., $M_L(n)$* or *$M_U(n)$*) depend on both the COM position and velocity, and illustrates how close the individual can be to loss-of-balance for the duration of a step. The smaller *M(n)* is the more probable loss-of-balance will be. A positive value is assigned to *M(n)* if the closest COM state to the ExFSR limits lies within ExFSR, and a negative value if the mentioned state lies outside the ExFSR (Figure 11). A negative *M(n)* is indicative of temporary loss-of-balance that needs to be recovered during the next step to prevent the incidence of falling. Based on the physiological condition of the walker and value of

negative *M(n)*, the temporary loss-of-balance can either be recovered or lead to an incidence of falling.

4.3.2 Experimental Protocol

To validate our proposed measures of stability against existing stability measures, we conducted a set of experiments using a CAREN [87]. 16 reflective markers were used to track the motions of the platform, body BOS, and body COM. We tracked the BOS motion using four makers mounted on a rigid plate attached to each foot. The body COM motion was tracked using four markers mounted on another plate attached over the sacrum. All the participants gave informed consent to perform the experiments approved by the local research ethics board (protocol number: Pro00066076). The same experimental data were used in [85]. 15 non-disabled individuals (body height: 179±9 cm and body weight of 78.7±5.8 kg; mean±standard deviation) and three individuals with amputation – one with unilateral trans-femoral, one with unilateral trans-tibial, and one with unilateral upper limb amputation and sustaining traumatic brain injury (body height: 179, 187, 168 cm, and body weight: 75.8, 79.7, 72 kg) – participated in this study. We recorded two 60-meter perturbed walking trials for each participant, a "low-perturbation" and a "high-perturbation" walking trial. During the low-perturbation (high-perturbation) trials, perturbations occurred in the form of vertical displacement and sagittal and lateral rotations of the BOS, with dominant frequencies and amplitudes of 1 Hz (3 Hz) and 1 cm (8 cm) in the vertical direction and of 1 Hz (3 Hz) and 0.06 deg (3 deg) in the rotational directions. Walking trials were performed on a treadmill, which adapted to the speed of walking of each individual to mimic natural walking. Normalized COM position and velocity with respect to the BOS at each instant were used to calculate the COM state trajectory. The ExFSRs for the duration of consecutive steps were obtained using the corresponding FSRs for each perturbation profile computed similar to [85] and the distance between the anterior edge of the posterior foot and posterior edge of anterior foot during the double-support phase.

4.3.3 Data Analysis

$M_L(n)$ and $M_U(n)$ was calculated for both lower and upper limits of the ExFSR and presented as an average among all steps in a walking trial ($M_{L,avg}$ and $M_{U,avg}$). In addition, for each step in each gait trials, we calculated other stability measures listed below to investigate potential correlations between them. The definition and symbol used for each stability measure are given in Table 3.

Table 3: List of our proposed measures of stability along with previously introduced measures of stability. Each measure's symbol, definition, and type (biomechanical or variability) have been presented.

Symbol	Definition	Type
$\boldsymbol{M_{L,avg}}$	Average of minimum distances[1] between the lower limit of ExFSR and COM state trajectory ($\boldsymbol{M_L(n)}$)[2] among all steps during one walking trial	Biomechanical
$\boldsymbol{M_{U,avg}}$	Average of minimum distances between the higher limit of ExFSR and COM state trajectory ($\boldsymbol{M_U(n)}$) among all steps during one walking trial	Biomechanical
$\boldsymbol{M_{L,neg}}$	Portion of steps in which $\boldsymbol{M_L(n)}$ is a negative value	Biomechanical
$\boldsymbol{M_{U,neg}}$	Portion of steps in which $\boldsymbol{M_U(n)}$ is a negative value	Biomechanical
$\boldsymbol{M_{neg}}$	Portion of steps in which $\boldsymbol{M_L(n)}$ or $\boldsymbol{M_U(n)}$ is a negative value	Biomechanical
$\boldsymbol{b_{min,avg}}$	Average of all b_{min} values during one walking trial	Biomechanical
$\boldsymbol{GCT_{MAD}}$	MAD[3] among all GCT[4] values during one walking trial	Variability
$\boldsymbol{GCT_{nMAD}}$	nMAD%[5] among all GCT values during one walking trial	Variability
$\boldsymbol{SPP_{MAD}}$	MAD among all SPP[6] values during one walking trial	Variability
$\boldsymbol{SPP_{nMAD}}$	nMAD% among all SPP values during one walking trial	Variability

Footnotes:

[1] A negative value if the COM state is outside of the ExFSR and otherwise a positive value

[2] n is the step number index

[3] *MAD* indicates the Median Absolute Deviation of parameter X among all steps of a walking trial: $MAD(X) = med(|X - med(X)|)$ (see [88])

[4] *GCT* indicates the gait cycle time

[5] *nMAD%* indicated the MAD normalized to the median value as a robust alternative to the coefficient of variation: $nMAD\% = 100 \times MAD/med$

[6] *SPP* indicates the swing phase percentage

Margin of stability based on the extrapolated centre of mass (XCOM): Hof et al. [15], [49] used an inverted pendulum model of the human body and suggested that, for dynamic stability of walking and standing, the body XCOM should remain within the BOS limits:

$$XCOM = P_{COM} + \frac{V_{COM}}{\omega_0} \quad , \quad \omega_0 = \sqrt{\frac{g}{l}} \qquad \text{(Eq. 4.1)}$$

where P_{COM} and V_{COM} are the body's COM position and velocity, g is the gravitational acceleration and l is the equivalent trochanteric length of each participant. They defined margin of stability (b) as the shortest distance between the XCOM and the BOS boundaries, and calculated it for every instant. The most unstable moment is when the value of b is minimum (b_{min}) within a step. We chose b_{min} because it is the most widely used biomechanical stability measure in the literature [9], [49], [89]. We calculated b_{min} for each step and considered the average of b_{min} among all steps ($b_{min,avg}$) as a measure of stability during a walking trial.

Variability measures: The variability of gait parameters such as Gait Cycle Time (GCT) and Swing Phase Percentage (SPP) has been introduced as an indicator of gait stability and risk of falling [90], [91]. To characterize the inter-stride variability of GCT and SPP, we calculated a robust measures, i.e., Median Absolute Deviation (MAD) [88] and normalized MAD (nMAD%), among all gait cycles of each walking trial (Table 3).

Correlation analysis: To investigate the relationship between variability measures, margin of stability based on XCOM, and our proposed margin of stability, we calculated (i) all above measures for the two perturbed walking trials of each participant; and (ii) the correlation coefficient between these measures among participants. We utilized Spearman's correlation coefficient because a monotonic relationship among the measures was expected.

4.4 Results

Since only three individuals with disability participated in this study, we did not perform statistical analyses between the groups. Nevertheless, the variability measures of stability (GCT_{cv}, $GCT_{MAD,}$ SPP_{cv}, and SPP_{MAD}) tended to be larger, and the XCOM-based measure of stability ($b_{min,avg}$) tended to be smaller for participants with disability compared to the non-disabled individuals for both low-perturbation and high-perturbation walking conditions (Figure 12) $M_{U,avg}$ tended to be smaller

for participants with disability compared to non-disabled individuals, in both conditions. However, $M_{L,avg}$ tended to be smaller for participants with disability only in the low-perturbation condition.

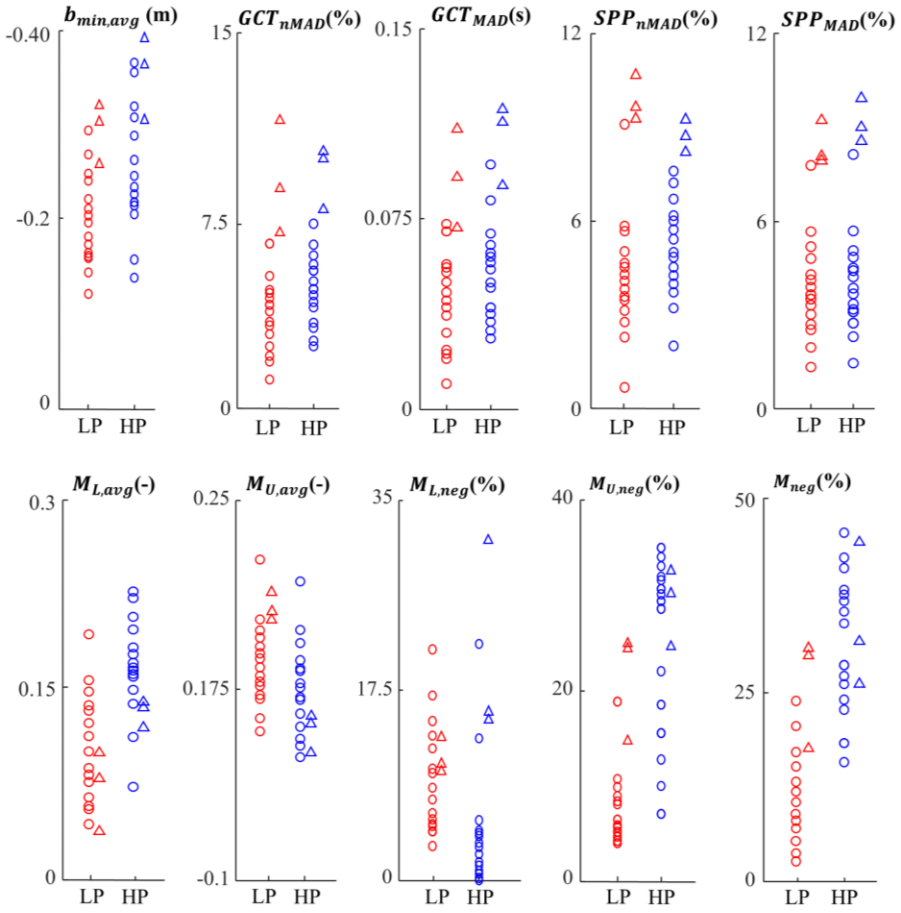

Figure 12: Stability measures obtained using experimental data. Our proposed measures ($M_{L,avg}$, $M_{U,avg}$, $M_{L,neg,}$ $M_{,U,neg,}$ M_{neg}), XCOM-based biomechanical measure ($b_{min,avg}$), and variability measures (GCT_{nMAD}, GCT_{MAD}, SPP_{nMAD}, and SPP_{MAD}) are presented for non-disabled participants (circle) and participants with disability (triangle), for low-perturbation (L_p, red) and high-perturbation (H_p, dark blue) walking trials.

The portion of steps in which the COM states were outside of the ExFSR limits, i.e., $M_{L,neg}$, $M_{U,neg}$, and M_{neg} (see Table 3), were 9.1% (4.6%), 7.2% (24.9%), and 11.1% (30.8%), respectively, in the low-perturbation (high-perturbation) condition for non-disabled participants. For the three

participants with disability, they were 12.2% (20.7%), 21.1% (29.3%), and 25.4% (33.3%). $M_{L,neg}$, $M_{U,neg}$, and M_{neg} tended to be larger for participants with disability.

For both perturbation conditions, $M_{L,avg}$ and $M_{U,avg}$ significantly correlated with $b_{min,avg}$. Unlike $M_{U,avg}$, the correlation coefficient between $M_{L,avg}$ and $b_{min,avg}$ was negative. Both $M_{U,neg}$ and M_{neg} significantly correlated with $b_{min,avg}$ in both perturbation conditions while $M_{L,neg}$ significantly correlated with $b_{min,avg}$ in only the low-perturbation condition. SPP_{MAD} significantly correlated with all $M_{L,\text{avg}}$, $M_{U,\text{avg}}$, $M_{L,neg}$, $M_{U,neg}$, and M_{neg} in the high-perturbation condition only. Also, SPP_{nMAD} significantly correlated with $M_{L,\text{avg}}$, $M_{U,\text{avg}}$, $M_{U,neg}$, and M_{neg} in the high-perturbation condition.

4.5 Discussion

In this study, we extended the use of FSR to an entire step composed of a swing phase and the following double-support phase during continuous walking, by defining the ExFSR. ExFSR consists of the FSR pertaining to both feet and space between them due to the distance between the heel of the swing foot and the toe of the standing foot. For a COM state trajectory starting from the toe-off instant of one foot and ending with the toe-off of the next foot (one swing phase and its succeeding double-support phase), if the trajectory lies within the ExFSR limits, no further balance recovery actions are required, whereas, if the trajectory passes these limits, a temporary loss-of-balance will occur. We defined measures of stability ($M_L(n)$ and $M_U(n)$) as the shortest distance between the lower and upper limits of ExFSR and the COM state trajectory, and their average among steps ($M_{L,avg}$ and $M_{U,avg}$). We also used the portion of steps in which the COM states went outside of the ExFSR limits, i.e., $M_{L,neg}$, $M_{U,neg}$, and M_{neg} (Table 4), as a means to validate our obtained ExFSR limits and stability measures.

Table 4: The correlation coefficients between our proposed measures of stability and previously introduced biomechanical and variability measures. In each cell, the correlation coefficient and the p-value for testing the hypothesis of no correlation (in parentheses) are presented. Significant correlations (p-value < 0.05) are bolded and shaded in grey. *Lp* and *Hp* stand for low-perturbation and high-perturbation walking conditions.

		$b_{min,avg}$	GCT_{nMad}	GCT_{MAD}	SPP_{nMad}	SPP_{MAD}
$M_{L,avg}$	***Lp***	**-0.41(0.02)**	-0.15(0.61)	-0.16(0.58)	-0.27(0.4)	-0.39(0.18)
	Hp	**-0.30(0.02)**	-0.04(0.90)	0.01(0.95)	**0.78(0.00)**	**0.72(0.01)**
$M_{U,avg}$	***Lp***	**0.60(0.02)**	-0.14(0.65	-0.11(0.73)	0.35(0.24)	0.35(0.24)
	Hp	**0.51(0.05)**	0.45(0.11)	0.37(0.22)	**0.62(0.02)**	**-0.65(0.02)**
$M_{L,neg}$	***Lp***	**0.70(0.01)**	0.31(0.31)	0.25(0.42)	0.23(0.45)	0.45(0.12)
	Hp	0.17(0.56)	-0.16(0.60)	-0.12(0.71)	0.26(0.37)	**-0.65(0.01)**
$M_{U,neg}$	***Lp***	**-0.59(0.03)**	0.11(0.71)	0.11(0.71)	-0.30(0.31)	-0.03,(0.91)
	Hp	**-0.54(0.05)**	-0.19(0.54)	-0.19(0.53)	**0.77(0.00)**	**0.65(0.01)**
M_{neg}	***Lp***	**-0.59(0.03)**	0.14(0.64)	0.11(0.71)	-0.30(0.32)	-0.12,(0.69)
	Hp	**-0.60(0.03)**	-0.32(0.29)	-0.22(0.47)	**0.83(0.00)**	**0.64(0.05)**

4.5.1 Validity and Relevance of Proposed Measures

Unlike $b_{min,avg}$, the ExFSR limits and consequently our proposed measures are a function of the perturbations or environmental conditions (such as slippage). Nevertheless, all stability measures defined based on *M(n)* significantly correlated with $b_{min,avg}$. These observations indicated the reliability of our proposed stability measures against the XCOM-based margin of stability. Note that $b_{min,avg}$ was considered as a reference since it is an established measure of dynamic stability in the literature [92], [93].

Our proposed stability measures enable us to characterize the biomechanical mechanisms of walking stability. We observed that $M_{L,avg}$ ($M_{U,avg}$) tended to increase (decrease) in high-perturbation walking trials compared to low-perturbation walking trials, especially for individuals with disability. In addition, unlike $M_{U,avg}$, the correlation coefficient between $M_{L,avg}$ and $b_{min,avg}$

was negative. This may indicate that, when the risk of loss-of-balance increases due to large external perturbations, the individual pushes the COM state away from the lower limit of ExFSR towards the more interior parts of ExFSR and closer to its upper limit to avoid a backward loss-of-balance. This can be justified since, unlike the backward loss-of-balance, the forward loss-of-balance can be recovered with taking extra steps forward. In other words, the neuromuscular control system tends to show more flexibility towards a forward loss-of-balance and chooses a larger distance to the lower limit of EXFSR. This effect was more dominant in impaired individuals because they tended to have a larger $M_{L,avg}$ and a smaller $M_{U,avg}$ compared to non-disabled individuals in high-perturbation conditions. Therefore, we recommend the use of both $M_{L,avg}$ and $M_{U,avg}$ for dynamic balance assessment. Nevertheless, the average of minimum distances between 'both' limits of ExFSR and COM state trajectory among all steps can also be a useful measure of stability when only one measure of stability is preferred. Although not presented, this measure significantly correlated with $b_{min,avg}$.

The portion of steps in which the COM states were outside of the lower and upper limits of ExFSR ($M_{L,neg}$ and $M_{U,neg}$) was 9.1% (4.6%) and 7.2% (24.9%) for non-disabled participants during low-perturbation (high-perturbation) conditions, and 12.2% (20.7%) and 21.1% (29.3%) for participants with disability during low-perturbation (high-perturbation) conditions. These measures tended to increase for participants with disability. Also, M_{neg} increases with perturbation level. Notably, observing a portion of COM states outside of the ExFSR limits cannot necessarily question the validity of our proposed stability measures. COM states outside of the FSR limits without an incidence of falling were also observed in previous works [85]. Indeed, a temporary loss-of-balance is usually recovered with various strategies, but their frequency could increase the risk of falling and, thus, we used $M_{L,neg}$, $M_{U,neg}$ and M_{neg} as measures of stability. In this line, we observed a correlation between $M_{L,neg}$, $M_{U,neg}$ and M_{neg}, and several other stability measures.

The calculation of our proposed measures only required measurements of the body COM trajectory and BOS motions, since the FSR limits are already formulated as a function of BOS perturbation in our previous work [85]. Reducing the number of variables required for balance assessment in clinical settings facilitates user-friendly methods of clinical balance assessment. Our experimental results included both non-disabled participants and participants with disability to show the

potential of our proposed stability measures to be utilized for both groups under various perturbation conditions.

4.5.2 Relationship with the Variability of Gait

In dynamical systems, increase in variability of the system's behavior can be associated with the instability and chaos in the system [58]. Variability measures have noticeable popularity among researchers in walking stability assessment, due to their simple calculation and understandable concept [13], [94]. Nevertheless, an increased variability in complex dynamical systems is not always indicative of chaos, but can also arise from the system characteristics and existence of multiple degrees of freedom in the system [58]. In low-perturbation walking trials, inter-stride variability of gait parameters can be due to a combination of both the system's internal dynamics and the external perturbation. Since these two effects could hardly be separated from each other, variability measures would be less meaningful [64]. In high-perturbation walking trials, the effect of the external perturbation on the dynamical system is amplified and, thus, variability measures are more susceptible to change. In this line, we observed correlations between the SPP variability and our proposed measures in the high-perturbation conditions only. The use of nMAD as a robust normalized variability index revealed correlation of SPP_{nMAD} with all our proposed measures, except for $M_{L,\mathrm{neg}}$. This could be in line with our hypothesis that the participants leaned their COM forward in high-perturbation conditions and, thus, despite the larger SPP visibility, the COM state trajectories do not more frequently go beyond the lower limit of ExFSR. In contrast to the SPP variability, the GCT variability did not correlate with our proposed measures. This could be due to the effects of the varying speed of treadmill on the inter-stride variability of GCT. In general, variability measures might not be reliable for stability assessment of perturbed walking conditions as it is not possible to separate the effects of external perturbation from the internal dynamics of the system. In addition, the non-stationary nature of gait parameter sequences due to external perturbation may cause overestimations of the variability measure.

4.5.3 Limitations

First, our proposed measures of stability are limited to sagittal plane movements of the body and BOS. However, the ExFSR limits are specific to the type of BOS perturbations. Similar to our previous study [85], to obtain the ExFSR limits, we only considered dominant BOS perturbations in the form of vertical displacement and sagittal rotation. Yet, the BOS perturbations in experimental data included lateral components that would affect the stability measures, which may explain a portion of the observed COM states outside of the ExFSR limits. A future prospective of our study is to determine the ExFSR limits for other types of BOS perturbation.

Second, our biomechanical model did not consider the effect of upper limb motion on balance recovery. Although the contribution of upper limb motion was neglected in several previous studies, it can modify the limits of loss-of-balance and the risk of falling, which should be studied in the future.

Third, in addition to biomechanical mechanisms discussed here, individual-specific physiological (e.g., muscle conditions) and cognitive conditions would affect the risk of loss-of-balance and falling [95]. Although our obtained ExFSR limits would contribute to developing strategies for prediction and prevention of falling, future work should characterize the individual-specific thresholds of our proposed measures for which loss-of-balance transitions to falling occur based on individual-specific measurements.

4.6 Conclusion

This study introduced a set of stability measures based on a previously developed seven-segment biomechanical model of the human body in the sagittal plane. These measures were able to characterize biomechanical mechanisms of loss-of-balance during perturbed and unperturbed continuous walking, as a function of BOS perturbation, and gait parameters (e.g., step length), and body motion pattern (e.g., COM states). The concept of ExFSR that was introduced for the first time in this study provides insight to margins of forward and backward loss-of-balance during

daily walking circumstances. Our proposed stability measures can contribute to our understanding on human balance control for biped walking, and the development of rehabilitative programs in interactive training environments such as the CAREN.

Chapter 5

5 Conclusions and future prospective

5.1 Main contribution and general results

We developed a biomechanical model of the human body in the sagittal plane that allowed us to determine the feasible stability region (FSR) during perturbed and unperturbed walking. This model consisted of seven segments including the feet, shanks, thighs, and head-arm-trunk (HAT) segments. We first used this model to obtain the FSR for the toe-off instant for unperturbed walking and showed that its result match those reported in the literature. We further subjected the base of support (BOS) of the model to external perturbations in the form of sinusoidal and obtained the FSRs for several perturbed walking circumstances with predetermined perturbation type, dominant frequency, and amplitude. We characterized the effects of perturbations frequency and amplitude over the limits of FSR and estimated these limits as a polynomial function of the frequency and amplitude of perturbations. Based on the shortest distance of the COM state and the limits of the obtained ExFSR for perturbed walking conditions, we introduced novel stability measures. Our proposed stability measures were capable of assessing the risk of loss-of-balance in perturbed and unperturbed walking conditions during an entire gait cycle and only required the measurement of COM and BOS motion. We collected experimental data from two groups of individuals; able-bodied participants and individuals with disability during unperturbed and perturbed walking trials with various levels and types of perturbation in the CAREN. We used the collected experimental data to investigate the validity of the obtained FSRs and ExFSR, and investigate the correlation between our proposed measure with other existing biomechanical and variability-based measures. We observed that specificity of our obtained FSRs and ExFSR for perturbed walking conditions was similar to those previously obtained for unperturbed walking. In addition, our proposed stability measures correlated with other existing biomechanical and variability-based measures in the literature. Therefore, they may contribute to our mechanistic

understanding on human balance control for walking affected by external perturbations, and to the development of rehabilitative programs in interactive training environments.

The original contributions of our study are summarized as follows:

1- **Revised optimization cost function for biomechanical modeling of walking**: The cost function that we utilized to conduct dynamic optimization in the simulations was adopted from a previous study by Yang et al [21]. However, we revised the previous cost function in order to make it suitable for simulating perturbed walking while maintaining realistic body postures throughout the simulated walking.
2- **Modeled BOS perturbation using a new approach**: Walking stability has already been analyzed in the literature only for a few perturbation conditions, such as slipping. However, walking during daily activities can be affected with various types of perturbations from various external sources. We modeled complex perturbation in the sagittal plane as a number of sinusoidal motions with different amplitudes and frequencies, and our model is capable of modeling other perturbations in the sagittal plane.
3- **Characterized FSR limits**: We estimated FSR limits as polynomial functions with coefficients depending on the type, frequency, and amplitude of the perturbations. Having these equations, one can obtain the FSR limits for an arbitrary set of frequency and amplitude of perturbation.
4- **Introduced the concept of Extended Feasible Stability Region (ExFSR)**: We introduced a new stability region based on the obtained FSRs for perturbed walking trials. ExFSR is valid for the whole duration of one complete step (toe-off to toe-off) and can be used for balance assessment of continuous walking.
5- **Introduced novel stability measures based on ExFSR**: We proposed a set of new stability measures based on ExFSR during perturbed walking. These measures can be obtained based on only COM motion states and BOS motion. The proposed measures have biomechanical signification, and the experimental data showed that they are correlated with the XCOM-based margin of stability and inter-stride variability of gait parameters.

5.2 Future prospective

5.2.1 Walking simulation in lateral and frontal planes

In the present study, we only considered body movements in the sagittal plane, and we neglected the movements in two other planes. Walking is a 3D motion, but literature has shown that the movements in the sagittal plane have more dominant effects on balance control. From our experimental observations, we found that even during forward walking, one can take a lateral step to recover his/her balance in the case of temporary loss-of-balance. The fact that we neglected movements in other planes is a limitation to our study, and future research can be conducted on developing a human body model to simulate gait motions in other planes and fusing the results with the results of the current study.

5.2.2 Investigating the effects of upper limbs

In the current study, we modeled the entire upper body as a rigid segment (HAT segment). Neglecting the upper limb segmentation equals to neglecting the motions of arms and head. Literature indicates that the effects and role of upper limbs motion in balance control during locomotion is not as dominant as the effects of lower limbs, but the fact that we neglected those motions is still a limitation to our study. Our rationale was to avoid adding extra joints and to reduce the computation cost to our model. Modeling the arms will add to the degrees of freedom and thus complexity of the model. A future study can be conducted to investigate the effects of upper limbs motions on FSR limits.

5.2.3 Simulate new perturbation profiles

Our developed biomechanical model has the capability of being subjected to any perturbation type in the sagittal plane. We are aiming to expand our horizon to other arbitrary perturbation profiles especially in the form of a combination of various perturbation types. Investigating multiple perturbation types and their effects on FSR limits will provide us with better insight into random

daily life perturbations. Developing a method to fuse the FSRs obtained from various perturbation profiles can be another future research topic.

5.2.4 Assessing the ability of an individual in balance recovery in the event of loss-of-balance

Knowing the limits of loss-of-balance allows us to monitor daily locomotion of individuals with walking disabilities and detect the instances where they lose their balance during their daily gait activity. Being able to quantitatively measure an individual's gait balance enables us to detect the thresholds of the quantitative measure where loss-of-balance transitions into incident of falling. Finding the threshold of the mentioned measure that separates falling from loss-of-balance also describes the ability of an individual in balance recovery at the event of loss-of-balance.

5.2.5 Developing training programs and guidelines for individuals with walking disabilities

Our obtained FSRs and stability measures can be utilized towards helping individuals with walking disabilities to identify their balance limitations and to hopefully overcome those limitations. Knowing the stability boundaries will allow us to provide individuals with guidelines and rehabilitation programs to reduce the risk of falling and injuries. Training programs can include exercises to help individuals learn their stability limitations and choose their walking patterns more efficiently. Our results can also be used towards designing walking models and step-placement predictions.

Bibliography

[1] D. Engelhart *et al.*, "Impaired Standing Balance in Elderly: A New Engineering Method Helps to Unravel Causes and Effects," *J. Am. Med. Dir. Assoc.*, vol. 15, no. 3, pp. 1–6, 2014.

[2] D. C. Mackey and S. N. Robinovitch, "Mechanisms underlying age-related differences in ability to recover balance with the ankle strategy," *Gait Posture*, vol. 23, no. 1, pp. 59–68, 2006.

[3] Division of Aging and Seniors, "Report on Seniors' Falls In Canada," Ottawa, Ontario, 2005.

[4] A. Stinchcombe, N. Kuran, and S. Powell, *Seniors' falls in Canada: Second report: Key highlights*, vol. 34, no. 2–3. 2014.

[5] D. Ganz, Y. Bao, P. Shekelle, and L. Rubenstein, "Will my patient fall?," *J. Am. Med. Assoc.*, vol. 297, no. 1, pp. 77–86, 2007.

[6] S. N. Robinovitch *et al.*, "Video capture of the circumstances of falls in elderly people residing in long-term care: An observational study," *Lancet*, vol. 381, no. 9860, pp. 47–54, 2013.

[7] A. Goswami *et al.*, "Compass-like biped robot Part I : stability and bifurcation of passive gaits," *RR-2996, INRIA*, 2006.

[8] Y. C. Pai and J. Patton, "Center of mass velocity-position predictions for balance control [published erratum appears in J Biomech 1998 Feb;31(2):199]," *J Biomech*, vol. 30, no. 4, pp. 347–354, 1997.

[9] S. M. Bruijn, O. G. Meijer, P. J. Beek, and J. H. Van Dieen, "Assessing the

stability of human locomotion: a review of current measures," *J. R. Soc. Interface*, vol. 10, p. 20120999, 2013.

[10] Y. Hurmuzlu, F. Génot, and B. Brogliato, "Modeling, stability and control of biped robots - A general framework," *Automatica*, vol. 40, no. 10, pp. 1647–1664, 2004.

[11] A. Wolf, J. B. Swift, H. L. Swinney, and J. A. Vastano, "Determining Lyapunov exponents from a time series," *Phys. 16D*, vol. 16, no. 3, pp. 285–317, 1985.

[12] A. D. Kuo, "Stabilization of lateral motion in passive dynamic walking," *Int. J. Rob. Res.*, vol. 18, no. 9, pp. 917–930, 1999.

[13] J. M. Hausdorff, D. A. Rios, and H. K. Edelberg, "Gait variability and fall risk in community-living older adults: A 1-year prospective study," *Arch. Phys. Med. Rehabil.*, vol. 82, no. 8, pp. 1050–1056, 2001.

[14] M. G. Pandy, "Computer modeling and simulation of human movement," *Kinesiology*, vol. 3, no. 1, pp. 245–273, 2001.

[15] A. L. Hof, "The 'extrapolated center of mass' concept suggests a simple control of balance in walking," *Hum. Mov. Sci.*, vol. 27, no. 1, pp. 112–125, 2008.

[16] F. Yang, D. Espy, and Y. C. Pai, "Feasible stability region in the frontal plane during human gait," *Ann. Biomed. Eng.*, vol. 37, no. 12, pp. 2606–2614, 2009.

[17] F. C. Anderson and M. G. Pandy, "Dynamic optimization of human walking," *J. Biomech. Eng.*, vol. 123, no. 5, p. 381, 2001.

[18] H. Hatze, "A comprehensive model for human motion simulation and its

application to the take-off phase of the long jump," *J. Biomech.*, vol. 14, no. 3, pp. 135–142, 1981.

[19] Y. C. Pai and K. Iqbal, "Simulated movement termination for balance recovery: Can movement strategies be sought to maintain stability in the presence of slipping or forced sliding?," *J. Biomech.*, vol. 32, no. 8, pp. 779–786, 1999.

[20] F. Madehkhaksar, J. Klenk, K. Sczuka, K. Gordt, I. Melzer, and M. Schwenk, "The effects of unexpected mechanical perturbations during treadmill walking on spatiotemporal gait parameters, and the dynamic stability measures by which to quantify postural response," *PLoS One*, vol. 13, no. 4, pp. 1–15, 2018.

[21] F. Yang, F. C. Anderson, and Y. C. Pai, "Predicted threshold against backward balance loss following a slip in gait," *J. Biomech.*, vol. 41, no. 9, pp. 1823–1831, 2008.

[22] W. T. Edwards, "Comments on 'Predicted region of stability for balance recovery: motion at the knee joint can improve termination of forward movement'.," *J. Biomech.*, vol. 34, no. 6, pp. 831–833, 2001.

[23] W. P. Berg, H. M. Alessio, E. M. Mills, and C. Tong, "Circumstances and consequences of falls in independent community-dwelling older adults," *Age Ageing*, vol. 26, no. 4, pp. 261–268, 1997.

[24] D. Zhao, J. Xu, D. Wu, K. Chen, and C. Li, "Gait definition and successive gait-transition method based on energy consumption for a quadruped," *Chinese J. Mech. Eng.*, vol. 25, no. 1, pp. 29–37, 2012.

[25] R. J. Jaeger and P. Vanitchatchavan, "Ground reaction forces during

termination of human gait," *J. Biomech.*, vol. 25, no. 10, pp. 1233–1236, 1992.

[26] C. P. Charalambous, "Repeatability of kinematic, kinetic, and electromyographic data in normal adult gait," *Class. Pap. Orthop.*, pp. 399–401, 2014.

[27] M. G. Pandy and T. P. Andriacchi, "Muscle and joint function in human locomotion," *Annual Review of Biomedical Engineering*, vol. 12, no. 1. pp. 401–433, 2010.

[28] G. Bergmann, G. Deuretzbacher, M. Heller, F. Graichen, and A. Rohlmann, "Hip contact and gait patterns from routine activities.PDF," vol. 34, pp. 859–871, 2001.

[29] D. A. Winter, *Biomechanics and motor control of human movement*. Hoboken, N.J.: John Wiley & Sons, 2005.

[30] V. T. Inman, "Human Locomotion," *Canad. Med. Assoc J*, vol. 94, no. 20, pp. 1047–1054, 1966.

[31] F. E. Zajac, "Muscle and tendon: properties, models, scaling, and application to biomechanics and motor control.," *Critical reviews in biomedical engineering*, vol. 17, no. 4. pp. 359–411, 1989.

[32] Y. Osaki, M. Kunin, B. Cohen, and T. Raphan, "Three-dimensional kinematics and dynamics of the foot during walking: A model of central control mechanisms," *Exp. Brain Res.*, vol. 176, no. 3, pp. 476–496, 2007.

[33] S. Scott, C. Engstrom, and G. Loeb, "Morphometry of human thigh muscles. Determination of fascicle architecture by magnetic resonance imaging.," *J. Anat.*, vol. 182, pp. 249–257, 1993.

[34] V. C. Mow and X. E. Guo, “Mechano-Electrochemical Properties Of Articular Cartilage: Their Inhomogeneities and Anisotropies,” *Annu. Rev. Biomed. Eng.*, vol. 4, no. 1, pp. 175–209, 2002.

[35] J. Baumgarte, “Stabilization of constraints and integrals of motion in dynamical systems,” *Comput. Methods Appl. Mech. Eng.*, vol. 1, no. 1, pp. 1–16, 1972.

[36] F. C. Anderson and M. G. Pandy, “A dynamic optimization solution for vertical jumping in three dimensions,” *Comput. Methods Biomech. Biomed. Engin.*, vol. 2, no. 3, pp. 201–231, 1999.

[37] M. G. Pandy, F. C. Anderson, and D. G. Hull, “A Parameter Optimization Approach for the Optimal Control of Large-Scale Musculoskeletal Systems,” *J. Biomech. Eng.*, vol. 114, no. 4, p. 450, 1992.

[38] A. M. Arruda-Olson, D. W. Mahoney, A. Nehra, M. Leckel, and P. A. Pellikka, “Cardiovascular effects of sildenafil during exercise in men with known or probable coronary artery disease: A randomized crossover trial,” *J. Am. Med. Assoc.*, vol. 287, no. 6, pp. 719–725, 2002.

[39] S. J. Piazza, “Muscle-driven forward dynamic simulations for the study of normal and pathological gait,” *J. Neuroeng. Rehabil.*, vol. 3, pp. 1–7, 2006.

[40] F. Yang and G. A. King, “Dynamic gait stability of treadmill versus overground walking in young adults,” *J. Electromyogr. Kinesiol.*, vol. 31, pp. 81–87, 2016.

[41] J. T. McConville, T. D. Churchill, I. Kaleps, C. E. Clauser, and J. Cuzzi, “Anthropometric relationships of body and body segments of inertia,” *AFAMRL*, vol. 80, no. 119, 1980.

[42] K. Terry, E. H. Sinitski, J. B. Dingwell, and J. M. Wilken, “Amplitude effects of medio-lateral mechanical and visual perturbations on gait,” *J. Biomech.*, vol. 45, no. 11, pp. 1979–1986, 2012.

[43] S. Roeles *et al.*, “Gait stability in response to platform, belt, and sensory perturbations in young and older adults,” *Med. Biol. Eng. Comput.*, no. Ml, pp. 1–11, 2018.

[44] K. P. Granata and T. E. Lockhart, “Dynamic stability differences in fall-prone and healthy adults,” *J. Electromyogr. Kinesiol.*, vol. 18, no. 2, pp. 172–178, 2008.

[45] J. B. Dingwell, H. G. Kang, and L. C. Marin, “The effects of sensory loss and walking speed on the orbital dynamic stability of human walking,” *J. Biomech.*, vol. 40, no. 8, pp. 1723–1730, 2007.

[46] B. E. Maki, P. J. Holliday, and A. K. Topper, “A prospective study of postural balance and risk of falling in an ambulatory and independent elderly population.,” *J. Gerontol.*, vol. 49, no. 2, pp. M72-84, Mar. 1994.

[47] M. R. Popović Pappas, I.P.I, Nakazawa, K., Keller, T., Morari, M., and Dietz, V., “Stability criterion for controlling standing in able bodied subjects.,” *J. Biomech.*, vol. 33, pp. 1359–1368, 2000.

[48] K. G. *et al.*, “The last station before fracture: Assessment of falling and loss of balance in elderly,” in *Turkiye Fiziksel Tip ve Rehabilitasyon Dergisi*, vol. 63, no. 1, 2017, pp. 14–22.

[49] A. L. Hof, M. G. J. Gazendam, and W. E. Sinke, “The condition for dynamic stability,” *J. Biomech.*, vol. 38, no. 1, pp. 1–8, 2005.

[50] Y. C. Pai, B. E. Maki, K. Iqbal, W. E. McIlroy, and S. D. Perry, “Thresholds

for step initiation induced by support-surface translation: A dynamic center-of-mass model provides much better prediction than a static model," *J. Biomech.*, vol. 33, no. 3, pp. 387–392, 2000.

[51] F. Yang, F. Saucedo, and M. Qiao, "Effects of a single-session stance-slip perturbation training program on reducing risk of slip-related falls," *J. Biomech.*, vol. 72, pp. 1–6, 2018.

[52] Y. Hurmuzlue and C. Basdogan, "On the measurement of dynamic stability of human locomotion," *J. Biomech. Eng.*, vol. 116, no. February 1994, pp. 30–36, 1994.

[53] N. Razali and A. Manaf, "Gait recognition using motion capture data," *Informatics Syst.*, pp. 67–71, 2012.

[54] A. Leardini, A. Chiari, U. Della Croce, and A. Cappozzo, "Human movement analysis using stereophotogrammetry Part 3. Soft tissue artifact assessment and compensation," *Gait Posture*, vol. 21, no. 2, pp. 212–225, 2005.

[55] A. Cappozzo, F. Catan, U. Della Crocel, and A. Leardini, "Position and orientation in space of bones during movement anatomical frame definition and determination," *Clin. Biomech.*, vol. 10, no. 4, pp. 171–178, 1995.

[56] C. J. Craig, *Introduction to robotics: mechanics and control*, 3rd Editio. New Jersey: Pearson, 2005.

[57] F. Yang and Y. Pai, "Can sacral markers approximate center of mass during gait and slip-fall recovery among community-dwelling older adults?," *J. Biomech.*, vol. 47, no. 16, pp. 3807–3812, 2015.

[58] D. J. Miller, N. Stergiou, and M. J. Kurz, "An improved surrogate method for detecting the presence of chaos in gait," *J. Biomech.*, vol. 39, no. 15, p.

2873—2876, 2006.

[59] M. T. Rosenstein, J. J. Collins, and C. J. De Luca, “A practical method for calculating largest Lyapunov exponents from small data sets,” *Phys. D*, vol. 65, pp. 117–134, 1993.

[60] J. B. Dingwell, “Differences Between Local and Orbital Dynamic Stability During Human Walking,” *J. Biomech. Eng.*, vol. 129, no. 4, p. 586, 2006.

[61] V. K. Jirsa, R. Friedrich, H. Haken, and J. A. S. Kelso, “A theoretical model of phase transitions in the human brain,” *Biol. Cybern.*, vol. 71, no. 1, pp. 27–35, 1994.

[62] J. M. Hausdorff, C. K. Peng, Z. Ladin, J. Y. Wei, and A. L. Goldberger, “Is walking a random walk? Evidence for long-range correlations in stride interval of human gait,” *J. Appl. Physiol.*, vol. 78, no. 1, pp. 349–358, 1995.

[63] T. M. Owings and M. D. Grabiner, “Step width variability, but not step length variability or step time variability, discriminates gait of healthy young and older adults during treadmill locomotion,” *J. Biomech.*, vol. 37, no. 6, pp. 935–938, 2004.

[64] N. Bernstein, *The coordination and regulation of movements*. New York: Pergamon Press, 1967.

[65] Y. C. Pai, B. Naughton, R. Chang, and M. Rogers, “Control of body centre of mass momentum during sit-to-stand among young and elderly adults,” *Gait Posture*, vol. 2, no. 2, pp. 109–116, 1994.

[66] A. L. Hof, “The equations of motion for a standing human reveal three mechanisms for balance,” *J. Biomech.*, vol. 40, no. 2, pp. 451–457, 2007.

[67] S. Wang, X. Liu, A. Lee, and Y. C. Pai, “Can recovery foot placement affect

older adults' slip-fall severity?," *Ann. Biomed. Eng.*, vol. 45, no. 8, pp. 1941–1948, 2017.

[68] I. P. Donald and C. J. Bulpitt, "The prognosis of falls in elderly people living at home.," *Age Ageing*, vol. 28, no. 2, pp. 121–125, 1999.

[69] J. A. Stevens and E. D. Sogolow, "Gender differences for non-fatal unintentional fall related injuries among older adults," *Inj. Prev.*, vol. 11, no. 2, pp. 115–119, 2005.

[70] G. A. R. Zijlstra, J. C. M. Van Haastregt, E. Van Rossum, J. T. M. Van Eijk, L. Yardley, and G. I. J. M. Kempen, "Interventions to reduce fear of falling in community-living older people: a systematic review," *J. Am. Geriatr. Soc.*, vol. 55, no. 4, pp. 603–615, 2007.

[71] Y. C. Pai, M. W. Rogers, J. Patton, T. D. Cain, and T. A. Hanke, "Static versus dynamic predictions of protective stepping following waist-pull perturbations in young and older adults," *J. Biomech.*, vol. 31, no. 12, pp. 1111–1118, 1998.

[72] Y. C. Pai, "Movement termination and stability in standing," *Exerc. Sport Sci. Rev.*, vol. 31, no. 1, pp. 19–25, 2003.

[73] A. D. Kuo, J. M. Donelan, and A. Ruina, "Energetic consequences of walkin Like an inverted pendulum: step to step transitions," *Exerc. Sport. Sci. Rev.*, vol. 33, no. 2, pp. 88–97, 2005.

[74] A. J. K. van Soest and L. J. R. R. Casius, "The merits of a parallel Genetic algorithm in solving hard optimization problems," *J. Biomech. Eng.*, vol. 125, no. 1, p. 141, 2003.

[75] S. L. Delp *et al.*, "OpenSim: Open-source software to create and analyze

dynamic simulations of movement," *IEEE Trans. Biomed. Eng.*, vol. 54, no. 11, pp. 1940–1950, 2007.

[76] F. Yang and Y. C. Pai, "Correction of the inertial effect resulting from a plate moving under low-friction conditions," *J. Biomech.*, vol. 40, no. 12, pp. 2723–2730, 2007.

[77] D. M. Jessop and M. T. G. Pain, "Maximum velocities in flexion and extension actions for sport," *J. Hum. Kinet.*, vol. 50, no. 1, pp. 37–44, 2016.

[78] Y.-C. P. Feng Yang, Frank C. Anderson, "Predicted threshold against backward balance loss in gait," *J. Biomech.*, vol. 49, no. 18, pp. 1841–1850, 2007.

[79] F. Yang, T. Bhatt, and Y. C. Pai, "Limits of recovery against slip-induced falls while walking," *J. Biomech.*, vol. 44, no. 15, pp. 2607–2613, 2011.

[80] J. B. Dingwell, J. S. Ulbrecht, J. Boch, M. B. Becker, J. T. O'Gorman, and P. R. Cavanagh, "Neuropathic gait shows only trends towards increased variability of sagittal plane kinematics during treadmill locomotion," *Gait Posture*, vol. 10, no. 1, pp. 21–29, 1999.

[81] D. S. Marigold, "Role of the unperturbed limb and arms in the reactive recovery response to an unexpected slip during locomotion," *J. Neurophysiol.*, vol. 89, no. 4, pp. 1727–1737, 2002.

[82] T. Herman, N. Giladi, T. Gurevich, and J. M. Hausdorff, "Gait instability and fractal dynamics of older adults with a 'cautious' gait: Why do certain older adults walk fearfully?," *Gait Posture*, vol. 21, no. 2, pp. 178–185, 2005.

[83] J. B. Dingwell, J. P. Cusumano, D. Sternad, and P. R. Cavanagh, "Slower speeds in patients with diabetic neuropathy," *J. Biomech.*, vol. 33, pp. 1269–

1277, 2000.

[84] A. L. Hof, S. M. Vermerris, and W. A. Gjaltema, “Balance responses to lateral perturbations in human treadmill walking,” *J. Exp. Biol.*, vol. 213, no. 15, pp. 2655–2664, 2010.

[85] H. Bahari, A. H. Vette, J. S. Hebert, and H. Rouhani, “Predicted threshold against forward and backward loss of balance for perturbed walking- Under review”, 2018.

[86] J. L. Patton, Y. C. Pai, and W. A. Lee, “Evaluation of a model that determines the stability limits of dynamic balance,” *Gait Posture*, vol. 9, no. 1, pp. 38–49, 1999.

[87] C. A. Rabago, J. B. Dingwell, and J. M. Wilken, “Reliability and minimum detectable change of temporal-spatial, kinematic, and dynamic stability measures during perturbed gait,” *PLoS One*, vol. 10, no. 11, pp. 1–22, 2015.

[88] T. Chau, S. Young, and S. Redekop, “Managing variability in the summary and comparison of gait data,” *J. Neuroeng. Rehabil.*, vol. 2, no. 22, pp. 1–20, 2005.

[89] P. M. McAndrew Young, J. M. Wilken, and J. B. Dingwell, “Dynamic margins of stability during human walking in destabilizing environments,” *J. Biomech.*, vol. 45, no. 6, pp. 1053–1059, 2012.

[90] J. M. Hausdorff, “Gait dynamics in Parkinson’s disease: Common and distinct behavior among stride length, gait variability, and fractal-like scaling,” *Chaos*, vol. 19, no. 2, 2009.

[91] V. Dubost, C. Annweiler, K. Aminian, B. Najafi, F. R. Herrmann, and O. Beauchet, “Stride-to-stride variability while enumerating animal names

among healthy young adults: Result of stride velocity or effect of attention-demanding task?," *Gait Posture*, vol. 27, no. 1, pp. 138–143, 2008.

[92] Y. Koyama *et al.*, "Relationships between performance and kinematic/kinetic variables of stair descent in patients with medial knee osteoarthritis: An evaluation of dynamic stability using an extrapolated center of mass," *Clin. Biomech.*, vol. 30, no. 10, pp. 1066–1070, 2015.

[93] A. T. Peebles, A. Reinholdt, A. P. Bruetsch, S. G. Lynch, and J. M. Huisinga, "Dynamic margin of stability during gait is altered in persons with multiple sclerosis," *J. Biomech.*, vol. 49, no. 16, pp. 3949–3955, 2016.

[94] S. Studenski *et al.*, "Gait speed and survival in older adults," *JAMA - J. Am. Med. Assoc.*, vol. 305, no. 1, pp. 50–58, 2011.

[95] C. P. Carty *et al.*, "Reactive stepping behaviour in response to forward loss of balance predicts future falls in community-dwelling older adults," *Age Ageing*, vol. 44, no. 1, pp. 109–115, 2015.

Appendix A

Ground reaction force underneath each foot was modeled using a series of spring-damper elements to model the distributed force. The distributed force was considered (rather than the resultant force) to precisely calculate the moments acting at the ankle joint due to the effect of ground reaction force. The vertical force of each element was modeled using the equations below:

$$F_{y,i} = Ae^{-1150(p_{y,i}-y_0)} - 100v_{y,i}g(p_{y,i}) \quad \text{Eq. A1}$$

$$g(p_{y,i}) = \frac{1}{1+10e^{500(p_{y,i}-g_0)}} \quad \text{Eq. A2}$$

Where $v_{y,i}$ is the vertical velocity of the point of application; A is a constant that is dependent on the number of springs used; $p_{y,i}$ is the vertical position of the point of application with respect to the ground surface; y_0 (= 0.0065905 m) is a parameter that determines when the magnitude of the spring force becomes significant (> 0.5 N); $g(p_{y,i})$ is an element that gradually brings damping in to effect as the foot gets closer to the ground surface; and g_0 (= 0.02 m) is a parameter that determines at which point damping starts.

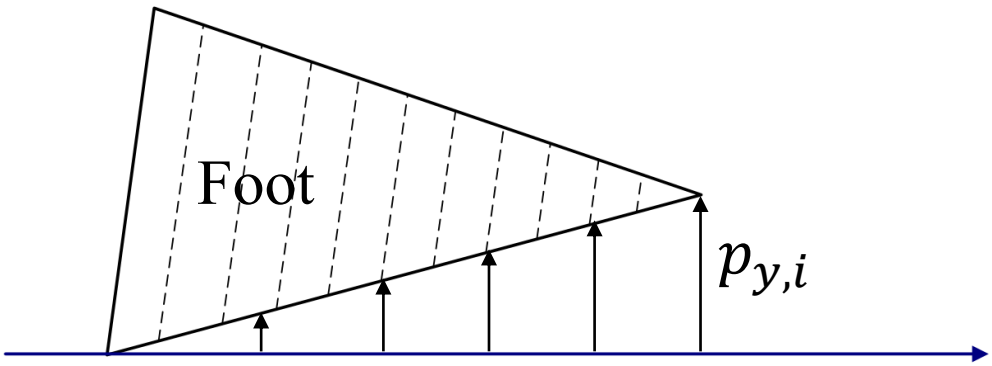

Figure A1: Schematic of ground reaction force modeling approach. Vertical arrows are indicative of spring-damper elements and their corresponding vertical force. Elements were spaced equally throughout the length of foot.